BUDAPEST UNIVERSITY OF TECHNOLOGY AND ECONOMICS

FACULTY OF MECHANICAL ENGINEERING

DEPARTMENT OF MACHINE AND PRODUCT DESIGN

ENGINEERING OF FRACTAL VISE: DESIGN AND INTEGRATION OF A HYBRID FRACTAL – BENCH VISE FOR ADAPTIVE CLAMPING OF IRREGULAR WORKPIECES

Author:

Muhammad Kevin Fahlevi

Supervisor:

Dr. Baka Ernő Zsolt

Gábor Vincze

STUDENT'S SCIENTIFIC CONFERENCE (TDK)

Budapest, 2025/26/1

ACKNOWLEDGEMENTS

First and foremost, I would like to express my sincere appreciation to the Maintenance Department of Atlas Copco PC Hungary for providing the resources and workspace necessary to build and carried out the manufacturing process for the prototype of this TDK project. I am especially grateful to my supervisor at the Atlas Copco, Mr. Gábor Vincze, for his continuous guidance, constructive feedback, and expert advice throughout this project. His technical knowledge and support have been instrumental in shaping my understanding of design engineering and project development.

I am also thankful to my engineering and technician colleagues, Mr. Marcell Mezei, Mr. János Lovász, and Mr. Iván Bagi for their kind cooperation and practical assistance in the workshop. Their insights and help with the tooling and installation process made essential contributions in the hands-on implementation of the design.

Special thanks to my supervisor from Department of Machine and Product Design, Dr. Baka Ernő Zsolt, whose encourages me to participate for the TDK competition and supervises during project documentation. His confidence in my abilities and motivation was my main driving force to complete the prototype and the paper.

This project would not have been possible without the collaborative spirit and mentorship I received, both from the industry and the university. I deeply appreciate the opportunity to develop my skills in such a supportive and professional environment.

Budapest, November 2nd 2025

Muhammad Kevin Fahlevi

ABSTRACT

The model variation of industrial vise, as a general work holding devices, has been increasing in recent years to reach numerous different styles of tool-clamping, ensuring its efficiency and durability. Bench Vise, for instance, can serve as a fundamental tool in machining, assembly, and manufacturing processes by ensuring that examined workpiece is securely held in place. This type of vise commonly experiences limitations of the inefficient gripping force when handling irregular, asymmetrical, or delicate components, resulting in uneven stress distribution, workpiece deformation, and surface damages such as scratches, dents, microfractures – reduces the quality and reliability of the manufactured parts.

To overcome these challenges, this paper introduces a mechanically hybrid vise system that integrates the adaptive clamping mechanism of a Fractal Vise, supported by the structural base and drive system of a Bench Vise. The main component applies a self-repeating arc structure inspired by fractal geometry, gradually decrease in size and dimension, enabling multiple contact points to adjust to complex cross-section while distributing pressure evenly. Dovetail mechanism is applied between the circular arcs components to enable sliding motion and pushes the smallest component (clamping jaws) to clamp the object securely.

The design process involves CAD modelling using *PTC Creo* while considering the application of DFM and DFA principles, *PET-G CF* for the additive manufacturing (3D printing) of the main fractal bodies, as well as *Aluminium* for the subtractive manufacturing (milling and turning) of the mounting interface, the connection plates between the Bench Vise and the Fractal Vise. Additionally, a prototype is produced using *Bambu Lab X1 Carbon Combo*, followed by mechanical testing and structural analysis to evaluate the clamping's performance, durability, and industrial usability.

Keywords: Fractal Vise, Bench Vise, Hybrid System, Adaptive Clamping, Irregular Workpieces, CAD Modelling, DFM/DFA, Additive Manufacturing, Substrative Manufacturing, Prototyping.

TABLE OF CONTENTS

1. INTRODUCTION

1.1 Problem Statement

The industrial vise has seen increased variations in recent years to improve tool-clamping efficiency and durability. The Bench Vise, commonly used in machining and assembly, for the purpose of workpiece-clamping in place. However, it often struggles with irregular or complex shapes of components, resulting to the inefficiency of gripping force and potentially causing uneven stress, deformation, and surface damage.

Inspired by the Fractal geometry, Fractal Vise uses fractal shapes to grip parts with many contact points, applicable for complex and unsymmetrical shapes of industrial tools [1]. The jaws which are built at the inner side of clamping area adjust to odd shapes and spread pressure evenly across the workpiece. Nevertheless, numerous design parameters, material selection for strength and durability, and different manufacturing processes (e.g. 3D printing, CNC machining) would lead to various types of application, thus initial action plan and design methodology such as DFM (Design for Manufacturing) and DFA (Design for Assembly) need to be considered.

This thesis aims to address these challenges by conducting a comprehensive study on the design, material selection, and manufacturing processes of the Fractal Vise, considering the material resources, manufacturing cost, shop-floor condition, and installation area. Experimental testing on several industrial tools at Atlas Copco Hungary also will be performed to evaluate the performance and usability of the product.

1.2 Objectives

This project began with the initial discussion on the design concept exploration where full assembly of general fractal vises will be designed, containing the following component divisions: mounting interface, central base block, driving arm, clamping jaws, fasteners and guide pins. The manufacturing processes followed with the analysis of different material options, including thermoplastics for prototyping via 3D printing and *aluminum* via milling and drilling processes

To optimize the usability of the available bench vise at the maintenance shop of Atlas Copco Hungary, it is discussed and agreed to design and manufacture the integrated system of two types of vises - a configuration in which the Bench Vise as a driving system provides the structural support, while the Fractal Vise acts as a clamping system, handles multi-point gripping mechanism. These integrated merged setups allowed us to utilize the available vise resource with the upgraded scale of application that conform to the shape of any object that it holds. In other words, the only components of Fractal Vise included are mounting interface, clamping jaws, fasteners, and guide pins as the bench vise body replaces the need of central base block, at the same time provides an original driving handle/arm.

Combining the clamping system of the Fractal Vise with the foundation and driving system of the Bench Vise saves installation space in the maintenance shop of Atlas Copco Hungary, as it prevents the need for a separate base block and handle system. It also simplifies assembly - considering the rectangular jaws of the Bench Visa can be disassembled - making the overall system easier to install, align, and operate. Moreover, using an existing Bench Vise also reduces material costs and shortens production time, while still achieving the self-adaptive clamping function for irregular-shape workpieces.

1.3 Thesis Outline

The structure of this thesis project is divided into the following chapters, elaborating the scope of work, testing evaluation in the maintenance operation point of view, and conclusion of this design discovery and its application.

- Chapter 1: Introduction

  Defines the research problem, explains motivation, outlines the objectives, states the scope of work, and presents an overview of the thesis structure.
- Chapter 2: Literature Review

  Describe the fundamentals of Fractal Geometry and its relevance to industrial clamping systems. Explores the existing types of Fractal vise, its strength and limitations in industrial practices.
- Chapter 3: Methodology

Presents the design approach of CAD modelling for the assembly, sub-assemblies' components, and individual parts of fractal and base plates, using PTC Creo. Describe the material analysis and selection motive for the fractal parts and mounting interface plates, examine thermoplastics for 3D printed prototypes and metallic materials for milling and drilling machined base plates. Elaborate the additive manufacturing for clamping jaws and subtractive manufacturing for mounting plates.

- Chapter 4: Results and Discussion
- Details the assembly process of the of fractal components onto the Fractal Vise, base plates components onto the mounting interface, and integration processes onto the Bench Vise. Display clamping tests, structural checks, stress and bending evaluations to validate functional performance. Evaluate structural analysis by applying Finite Element Analysis (FEA) using SolidWorks simulation to describe model stress, strain, deformation, and load-bearing performance under typical working conditions.
- Chapter 5: Conclusion

  Summarizes key findings, validates the design solution, and reflects on the Atlas Copco Maintenance team contributions to improving work holding systems in manufacturing

2. LITERATURE REVIEW

2.1 Background of Fractal Geometry

Fractals are geometric patterns that repeat at every scale, forming structures that appear similar no matter how closely the shape zoom in – a pattern that never ends [2]. The concept was formalized by Benot B. Mandelbrot (French-American mathematician) in 1980 through *the Mandelbrot Set* – a complex two-dimensional plot showing which complex numbers remain bounded when iterated by the formula $z_{n+1} = z_{n^2} + c$, where both z and c are complex numbers. This property of repeating structure is called self-similarity [3].

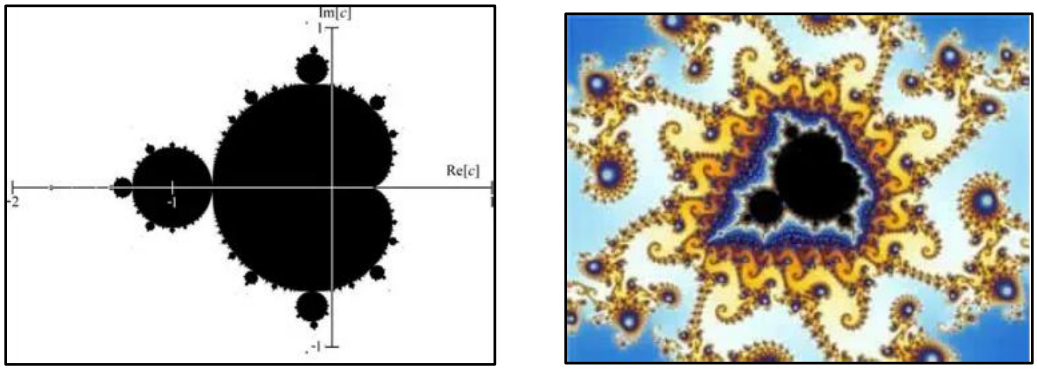

Picture 1. Graph of Mandelbrot Set and fractal geometry visualization

Fractals are not just mathematical objects; they also occur widely in nature. Examples include three branches, snowflakes, coastlines, succulents, crystals, and pinecones [4]. Natural fractals often form spirals or repeating patterns, like broccoli florets that resemble the whole head. This growth follows a spiral shaped by the golden ratio *phi (φ)*, producing taller tips as the structure expands.

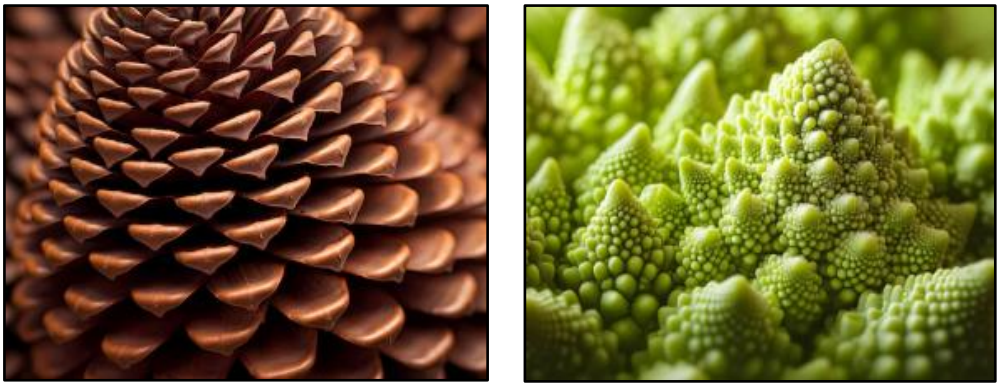

Picture 2. Fractal shapes of Pinecones and Romanesco Broccoli

Fractal geometry has revolutionised how complex systems are understood. Its concepts are now applied across many fields – such as dynamical systems, probability and statistical mechanics. To explain phenomena like matter distribution in the universe, turbulence fluid flow, and even the generation of realistic textures and natural-looking landscapes. Traditional Euclidean geometry often fails to represent the irregular shapes and complex forms seen in nature. Fractal geometry, with its emphasis on scaling and self-similarity, offers a more accurate means of modelling natural structures. This principle inspired the design of the Fractal Vise: each-semi claw body follows a fractal-based pattern.

2.2 Principle of Fractal Vise

Fractal Vise is a unique industrial clamping tool that uses fractal-based geometry to adapt to the of the object it grips [5]. As shown in Picture 3, it showcases a custom contact surface made of circular arcs that adjust to the workpiece's shape. Similar to the characteristics of fractal shape, its design follows an iterative, self-repeating pattern which built from arcs, gradually decrease in size and dimension. By applying the tapering curvature, the vise could strongly hold objects while applying even and gentle pressure; suitable for handling parts with diverse shapes.

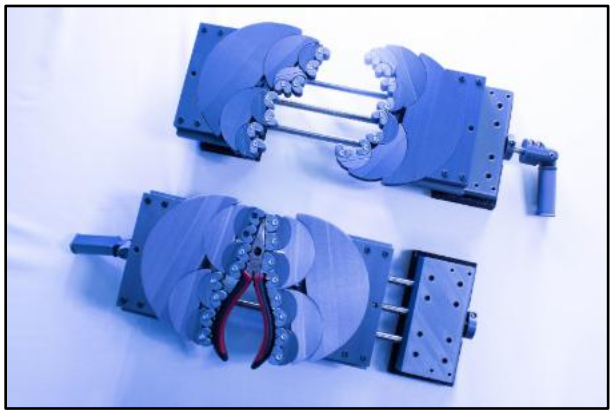

Picture 3. Fractal Vise with and without examined workpiece

The main semi-circle body of Fractal Vise applies a series of concentric arcs, where each arc is about half the size of the arc prior to it, as shown in the figure below. When the outer jaws exert force to the workpiece, the sliding dovetail joints enable each arc to rotate and conform to the natural shape of the object.

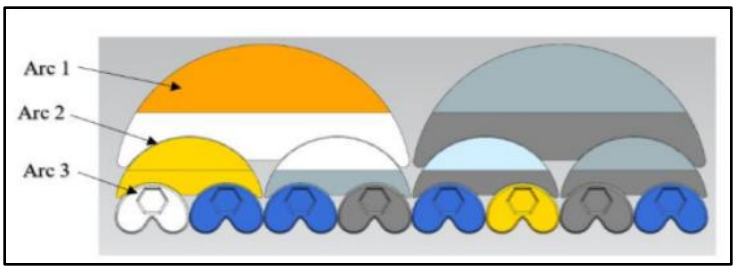

Picture 4. Fractal Vise with and without examined workpiece

The vise system consists of ten essential parts. The operation begins with the user rotating a crank (1), converting rotational motion through the nut into liner motion via a lead screw (2). This drives a half-rectangular block (3), containing the dovetail mechanism forward. Components (8) and (3) are symmetrical, connected by arcs of equal diameter. When the smallest arc (6) contacts the object, the connected parts (3), (4), (5), (6), and (7) follow the movement through the groove system and shape themselves to fit the workpiece's surface precisely [5].

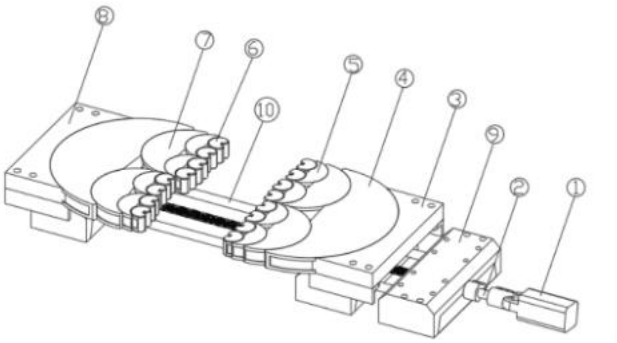

Picture 5. Mechanical structure of the general Fractal Vise

To keep the object securely in the gripping area, the generated friction force between the vise and the examined component must be larger than the part's weight (W) [5]. This friction force relies on the clamping force (F_h) applied by the vise. The clamping conditions must meet the following requirement:

$$Ff = \mu N = \mu Fh > W$$

Where W is the workpiece's weight and F_f is the friction force. The coefficient of friction denoted by μ is 0.2.

Since the manufactured Fractal Vise is used for relatively small or medium-shaped tools, the average mass of the examined workpiece is about 1-2 Kg. 2 Kg mass equals to *19.62 N* weight, as calculated by the following equation:

$$W = M \cdot g \; W = M \cdot g$$

With the *19.62 N*, the minimum clamping force F_h must be greater than *98.1 N* or rounded to *100 N*. The vise will also experience a reaction force $N=F_h=100\ N$ and the friction force F_f is calculated [6]:

$$Ff = \mu N = \mu Fh = 0.2 \cdot 100 = 20\,N \; Ff = \mu N = \mu Fh = 0.2 \cdot 100 = 20\,N$$

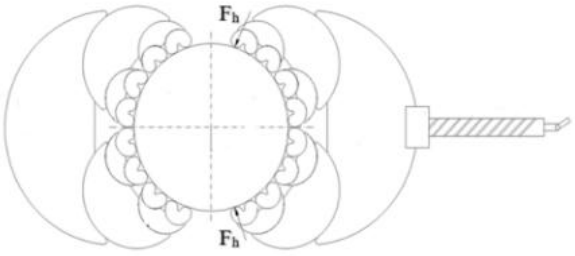

Picture 6. Clamping model

Consider *PETG – CF* is the material used to produce the Fractal components, the tensile strength at yield σ_y is *57.6 MPa* (ISO 527). Given the safety factor SF for the 3D printed parts (anisotropic, layer based) of 2 is standard, the allowable stress σ_{allow} can be obtained by:

$$\sigma allow = \sigma ySF = 57.62 = 28.8 \sim 29\,MPa, \sigma allow = \sigma ySF = 57.62 = 28.8\,MPa$$

The minimum cross-sectional area A of the clamping jaw is determined as follows:

$$A = N\sigma allow \cdot SF = 10029 \cdot 2 = 6.9\,mm2$$
$$A = N\sigma allow \cdot SF = 10029 \cdot 2 = 6.9\,mm2$$

A represents the contact area between the Fractal jaws component and part. The cross section of this component is shown below:

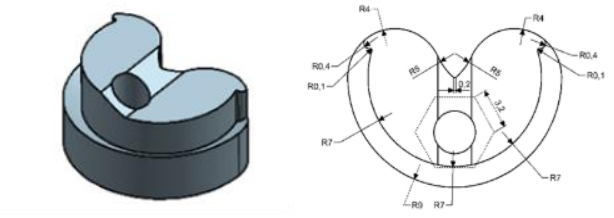

Picture 7. Clamping jaws component

2.3 Classification of Fractal Vise

Currently there are various type of Fractal Vise design variations in the market, which each manufacturing or maintenance shopfloor might use different design depending on their application and scalability [7]. In terms of design features, Fractal Vises can be categorized based on their power mechanism, jaw's structure, and tooth design.

2.3.1 Classification Based on Power Mechanism

The mechanism of clamping force generation is one of the key differences among Fractal Vises. Similar to a standard Bench Vise, the first type of driving mechanism applies a rotating handle. In general, the clockwise direction is used to turn the handle which drives a lead screw, converting rotational input from the user into a linear motion to the vise jaws. Considering its simplicity, easily controlled, and efficient for industry installation; from light-duty clamping to heavy machining, depending on the material used, this power mechanism approach is universally applied among the industry.

Picture 8. Rotating-handle Fractal Vise

Another power-mechanism variant is the gear-driven Fractal Vise; applied interlocking gears system instead of a lead screw. The fractal jaws clamp and move together in synchronize motion while the user rotates the gear. Practically in the compact design, the user can exert less effort with the higher torque transmission. This approach is significantly advantaged in automated or high-precision environments.

Picture 9. Rotating-gear Fractal Vise

2.3.2 Classification Based on Jaw Structure

The jaw structure of a Fractal Vise defines how contact points engage with the workpiece and distribute forces. Common designs use mechanical-bearing types with pivot joints or pins, which make segments to rotate and adapt to various shapes. These systems offer strong grip and rigidity while minimizing wear in tight areas, especially around metal components [8].

Alternatively, flexure-based jaws use flexible elements that bend slightly to match surface contours. While lightweight and low-maintenance – ideal for delicate tasks – these jaws present less clamping force and can fatigue over time which lead them more suitable for low-load applications.

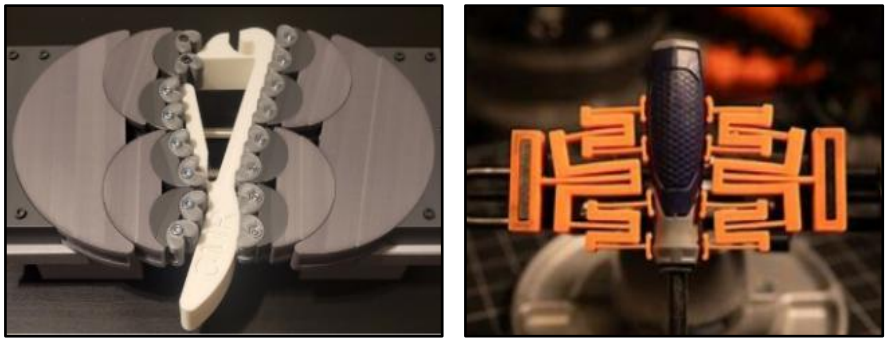

Picture 10. Mechanical bearing jaws (left) and Flexure jaws (right) of Fractal Vise

2.3.3 Classification Based on Teeth Design

While the engineer choses mechanical bearing jaws to be manufactured for the industrial application, there are some additional considerations of specific teeth design which built with the structure of mechanical-bearing jaws. The teeth design can vary depending on the intended contact with the examined object [9]. The first model is flat-surfaced teeth, which is more appropriate for rectangular or cubic-formed workpieces. This model type is the easiest design to manufacture and cost-effective option for flat-surfaced metalworking, but less-effective when used with round or uneven shapes.

The second version uses C-shaped jaws, which specifically modelled for cylindrical industrial tools such as pipes and tubes. By implementing the concave shape, this design helps prevent slippage or rolling during clamping, at the same time expands area of the contact surfaces.

The third and most versatile design in the market as well as in the industrial environment is curved jaws with semi-circular profiles. Multiple contact points are generated within this model and adjust more naturally to a variety of shapes, involving flat, round, or curved surfaces. The benefit of this approach is better vibration control and more uniform force distribution [10]. Since the jaws shapes are more complex compared to the first two shapes – flat and C jaws – manufacturing wise can be the most challenging and its performance may be slightly lower when clamping large flat surface which is better with the flat-jaws Fractal Vise. When it's made of metal, the extra movement in the pivoting joints may also result in higher long-term wear.

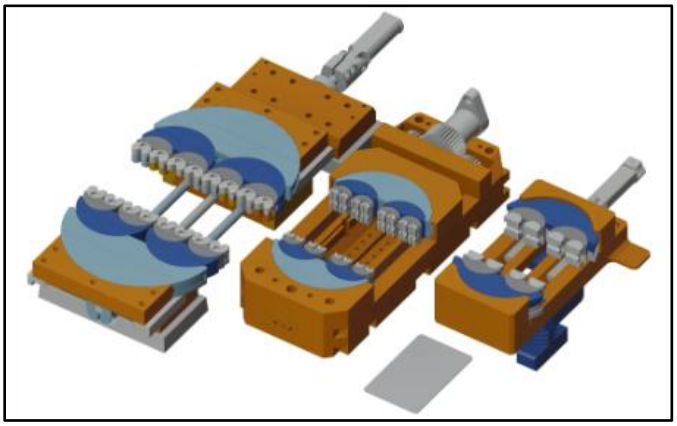

Picture 11. Various teeth designs of Fractal Vise

3. METHODOLOGY

3.1 CAD Design and Modelling

This chapter describe the design process via *PTC Creo* of full-integration assembly of the hybrid vise system, sub-assemblies' components (e.g. mounting interface assembly and Fractal Vise assembly), and each arc of fractal components which built the main function. The modelling of mounting interface and Fractal Vise was carried out from scratch by considering the installation space on the available Bench Vise at the maintenance shopfloor, meanwhile the CAD model of Bench Vise is taken from the market or engineering catalogue which has the same version to the installed device.

3.1.1 Vise Integration Assembly

The main assembly shows how the Fractal Vise is being integrated or assembled into the Bench Vise as a support base system, with the connection of the mounting interface. The models illustrate how the fractal jaws are mounted on a custom base structure, which links directly to Bench Vise's jaws. There are two variant models of the full integration assembly which are the initial model and upgraded model, based on the sub-assembly design of the mounting interface plates.

The first or initial assembly model of integration assembly contains three base plates (two vertical and one horizontal orientation) as a linking connector between both vises. This served as an original and testing configuration to evaluate the orientation and stability of the base plate's connection to the Bench Vise. This version is initially adequate for basic application on the industrial tools, but during manual testing, it was identified that the bottom sides of both Fractal Vise jaws assemblies slightly began to bend when very high force was applied to the jaws. In short, a second variant was modelled using an additional one horizontal plate which covers half of the top surface of the Fractal Vise jaws to prevent upward bending during application. Therefore, the change of the upgraded version was specifically on the mounting interface where in total four base plates are used (two vertical and two horizontal orientation).

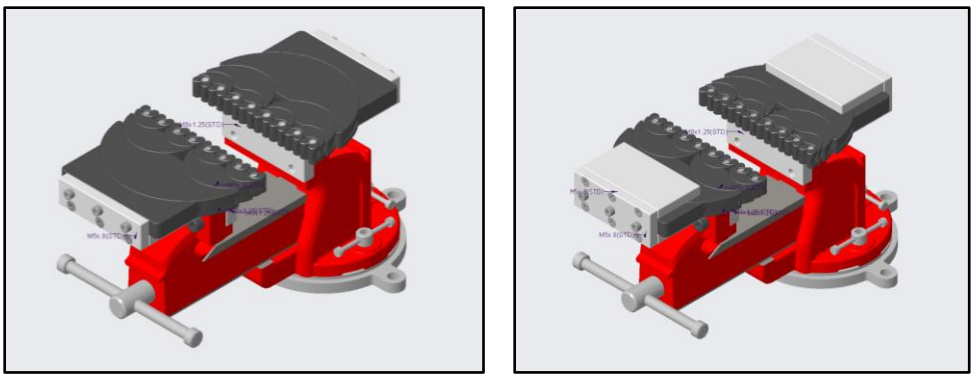

Picture 12. Model 1 - original (left) and model 2 - upgraded of vise integration assemblies

In this vise integration assembly, two types of standardized screws are used to ensure secure connections between the mounting interface components and the Fractal Vise or Bench Vise body. Countersunk screws are used to assemble the base plates; 12 pcs were applied in the first model and 18 pcs in the second or upgraded model. The second screw, counter bore socket head cap screws are installed for the connection between the Aluminium base plates and the clamping parts of Fractal Vise (M5x16), as well as connection the Bench Vise where higher torque and strength are needed due to the greater load (M8X25). These screws are ISO-standard and are frequently applied in mechanical design due to their high tensile strength and reliability in resisting shear and axial force.

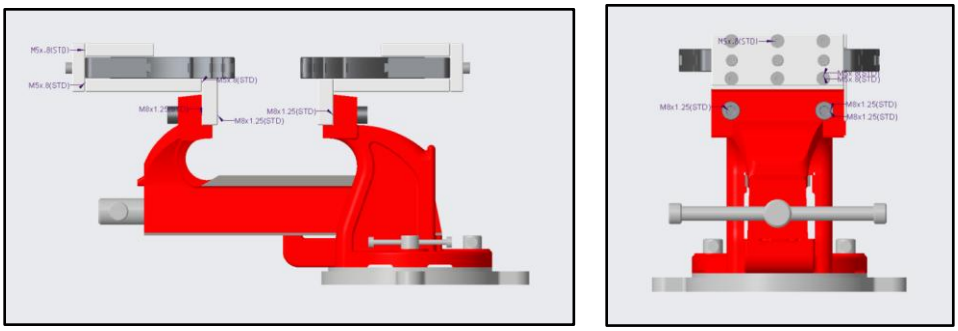

Picture 13. Right and front views of the vise integration assembly – upgraded

The section view below (Picture 14) illustrates the complete fastening system of one-half assembly after all screws are fully installed across the mounting interface and Fractal Vise assembly. On the left side, four M5X16 screws are shown attaching the main clamping components of the Fractal Vise to the aluminium base plates. Since these Fractal components are fabricated

using thermoplastic composite materials (PETG – CF), traditional internal threading via 3D printing is mechanically unreliable due to poor resolution and low thread strength. To resolve this, threaded brass inserts model from the online source were installed into pre-designed flat holes in the plastic parts. These inserts act as a metallic anchoring points for the screws. Each insert has a length of 10 mm, an inner diameter of 4.13 mm suitable for M5 screws, and an outer thread pitch diameter of 8 mm to ensure firm engagement with the plastic body. The inserts were embedded using a heat-set or press-fit method to guarantee safe holder under repetitive loading. This approach not only reinforces the thermoplastics' fastening capacity but also obstructs thread stripping, a common issue with polymer-based assemblies under torque or vibration. On the right side of the section view, two M8X25 socket head screws are used to fix the mounting base plates to the vertical surface of the Bench Vise, secure via threaded holes to ensure full rigidity of the upgraded model.

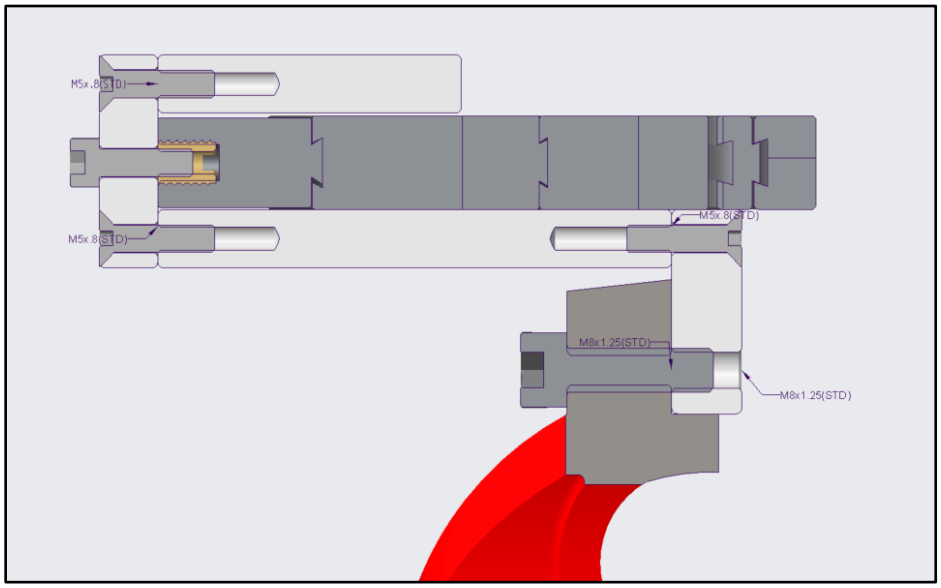

Picture 14. Cross-section view of the screw's connection within the vise integration assembly – upgraded

This exploded view below illustrates the sequential assembly of the upgraded vise integration system, clearly displaying how each individual component aligns along the vertical axis during the assembly process. From bottom to top, the image emphasizes the hierarchical positional of the main Bench Vise (in red), the mounting interface base plates (in white), and the Fractal Vise modules (in black). This configuration reinforces how mechanical fastening been instrumental in unifying diverse material components – cast iron, aluminium ally, and thermoplastic composite –

into a single functional system. Each fastening is labelled with its respective screw specification, such as M8x1.25 (STD) or M5X0.8 (STD), allowing for clear traceability of installation steps.

In addition, this visualisation is beneficial for checking design clearance, particularly between overlapping geometries and countersunk/tapped regions. The use of exploded spacing provides insight into how each layer depends on underlying structural support, especially the interface between the Fractal Vise and the Aluminium base, which is reinforced by multiple screw insertions for load bearing and alignment precision. By isolating each sub-assembly, this exploded view also facilitates error checking during manufacturing or assembly by making each interaction between components visually explicit.

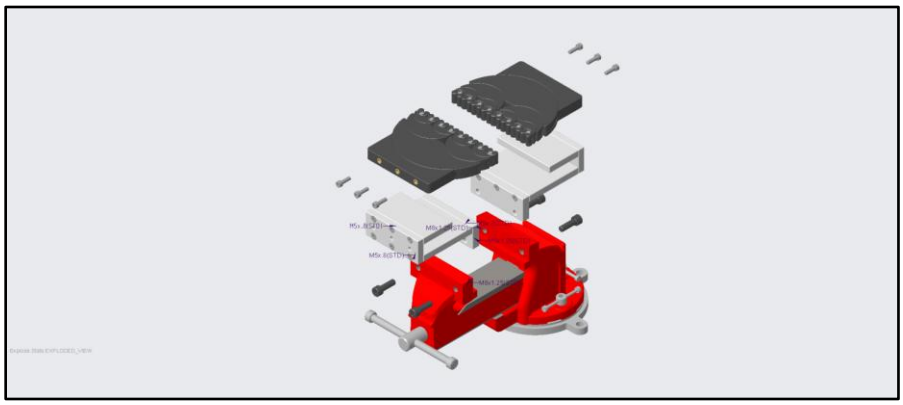

Picture 15. Exploded view model of the vise integration assembly – upgraded

In the final assembly drawing shown below, the total length of the entire assembly is 350 mm, with a working platform span of 295 mm. This distance corresponds to the maximum lateral coverage of the Fractal Vise jaw assemblies. The height from the base to the uppermost jaw surface is 182 mm, with the height of the Bench Vise from the base is 141 mm. The dimension of 325 mm from the base support to the front end of driving handle reflects the complete spatial footprint of the installation.

The right-side orthographic view reveals the top face of the Base Plate assembly, where the six screw holes (M5x16) fix the Fractal Vise to the Aluminium base, arranged in two rows of three to maintain the balance load distribution. Meanwhile, the side view displays the positioning area of 50 mm for the examined workpiece, between two clamping jaws of Fractal Vise. However, in real life, this distance of clamping area really depends on how much the movable jaws of

Bench Vise can be pulled to the backside. Normally, the distance is in range of 100 – 150 mm, where for the Bench Vise at Atlas Copco shopfloor, the length of middle space is approximately 140 mm, with a width of 130 mm. The number of hexes. Socket head screws for M5x6 are six pieces, followed by 4 pieces of M8X25.

The 3D rendering in the bottom-left corner of the drawing gives a visual correlation between the components, making it easier to interpret how each element fits and aligns in physical space. All dimensions and scale values (2:5 for the main drawing and 1:5 for the 3D isometric view) are defined based on standard A4 drawing practices using Creo software.

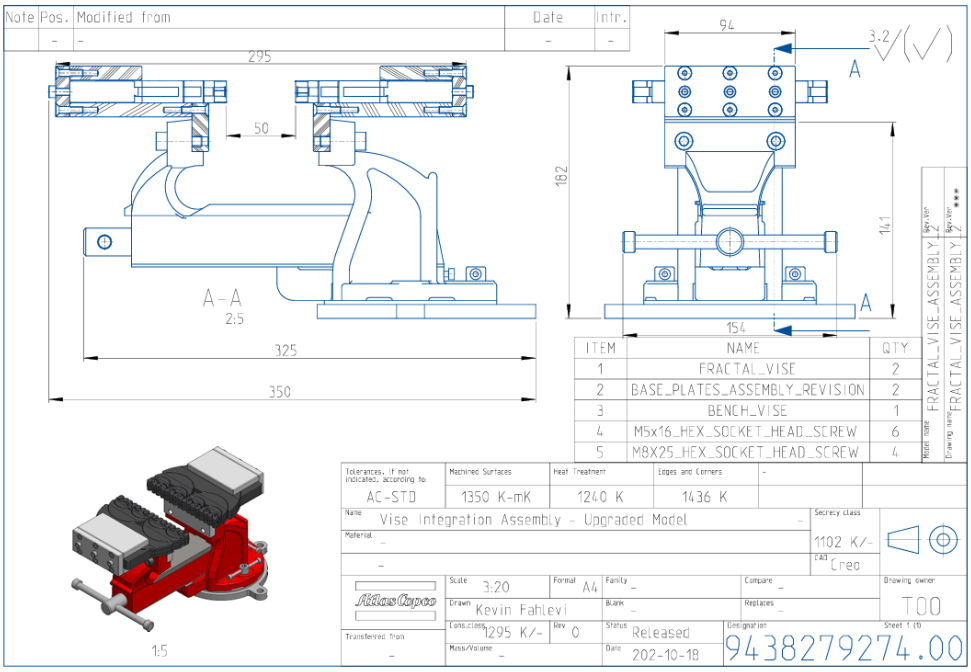

Picture 16. Assembly drawing of the vise integration assembly – upgraded

3.1.2 Mounting Interface Assembly

The role of the mounting interface within the overall integration assembly is to connect the main clamping components from the Fractal Vise and the support base and driving system from the Bench Vise. This component is the key part where the full integration assembly was divided into two variants. Three base plates were used in the first model and four base plates in the second

or upgraded version. The dimensions for each base plate were taken based on the approximation measurements directly on the Bench Vise at the maintenance shop floor, using a digital caliper.

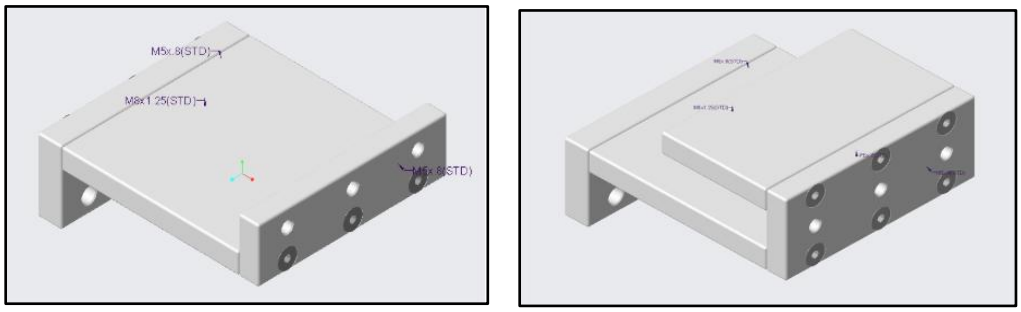

Picture 17. Model 1 (left) and model 2 (right) of mounting interface assemblies

From the model above, one horizontal support or cap on the model two which length half of the main platform where the Fractal Vise is placed. This length is sufficient to hold and maintain the stability of the main clamping components under high forces and pressures. Aside from that, every plate is connected through the countersunk screws M5x20 where three fasteners are used between two plates which spread with equal lengths to each other. From the exploded view model below, the mounting system clearly demonstrates how each countersunk screws are connected form a rigid unit. Within this assembly model, 9 countersunk screws are used in total, but this has not included the screws to mount the Fractal Vise with the base plate as well as to integrate this part to the Bench Vise. The use of countersink heads lets the screws sit below the surface level, preventing interference with other components during clamping.

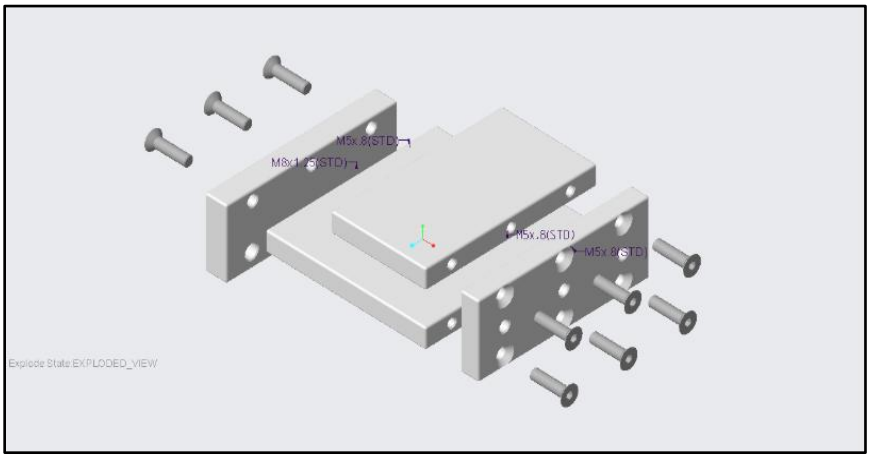

Picture 18. Exploded view model of upgraded mounting interface assembly

The design of vertical base plate 1 as a connecting plate to the Bench Vise exemplifies the modelling approach used for all base plates in this assembly. The design process began with a simple rectangular base profile created using *Sketch 1* with 94 mm x 12 mm and extruded to 35 mm tall. Following this, two main sets of features were added: simple-drilled and counter-sink holes (Ø5.2 mm) to connect with the horizontal base plate using M5 screws, and two threaded holes of M8x1.25 to fasten the assembly directly to the Bench Vise. Threaded specifications were defined using the ISO standard with sufficient depth. For safety, 1 mm rounds and 0.5 mm chamfers were applied to sharp edges, while a groove cut was modeled for mechanical alignment. Since all other base plates in the assembly follow a similar modeling methodology – defined by sketches, extrusions, and hole features – this plate is presented as a representative example to illustrate the overall design process used.

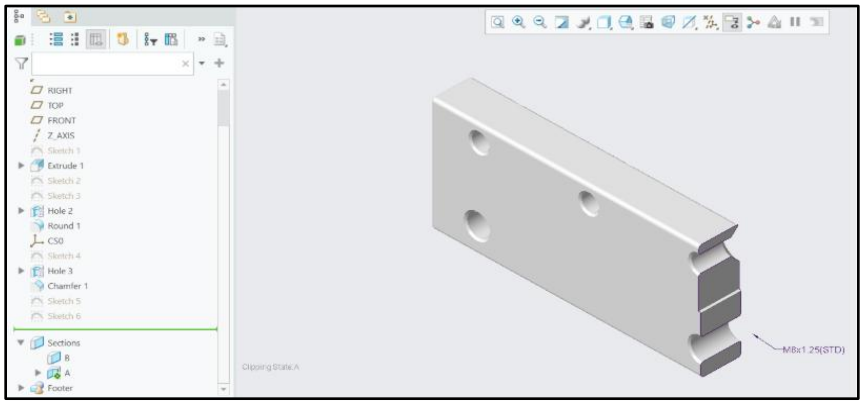

Picture 19. Model of base plate 1 – half view half cross-section

In the assembly drawing of the upgraded mounting interface model, the full geometry and key specifications of the component are laid out in detail. One of the most important features of this assembly is the series of simple drilled holes with a 5.2 mm diameter, as indicated on the front view. These three holes are positioned in pairs across the length of the plate, accurately spaced to accommodate M5 screws. Their main purpose is to allow the positioning of the Fractal Vise onto the mounting interface. In addition to the 5.2 mm holes, a second set of holes is shown both in the front view and side view. These are M8x1.25 STD (Standardized) standard straight-drilled holes with 6.8 mm diameter, used for connecting the base plates together with the Bench Vise body, particularly where the rectangular jaws of Bench Vise are placed. This will be connected using the original screws from the Bench Vise.

The total length of the part is 110 mm, with a total height of 61.5 mm. Each base plate has different values of height, considering the thickness of Fractal Vise and height of the jaws area on the Bench Vise. The first vertical base plate which connects to the jaws of the Bench Vise has 35 mm height and the third base plate has height 36.5 mm. 0.5 mm tolerance was made for the small gap area between the Fractal Vise and the second base plate to let the semi-columns components slide through its path without any friction. The wall thickness of each plate is 10 mm with the total weight of the full mounting interface assembly is 489 grams, roughly half a Kilogram, which supports the lightweight but rigid character of Aluminum 99.5 for this part.

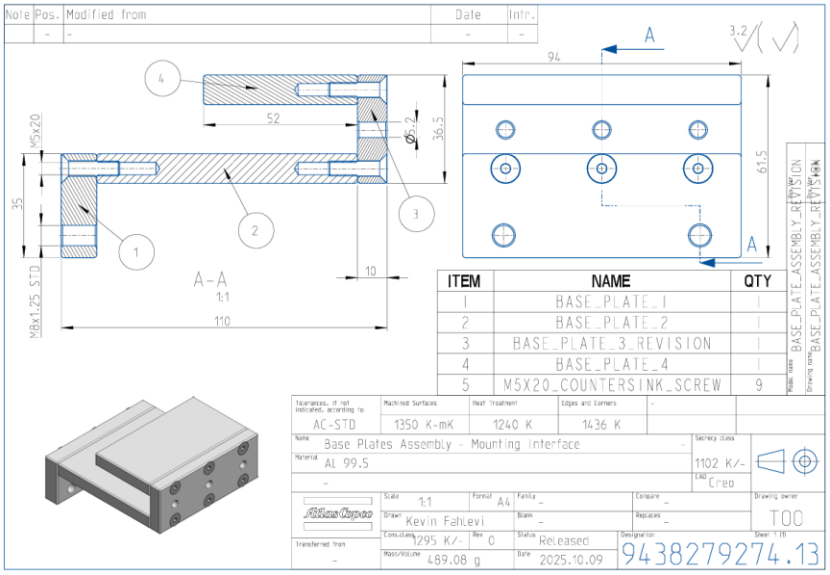

Picture 20. Assembly drawing of upgraded mounting interface assembly

3.1.3 Fractal Vise Assembly

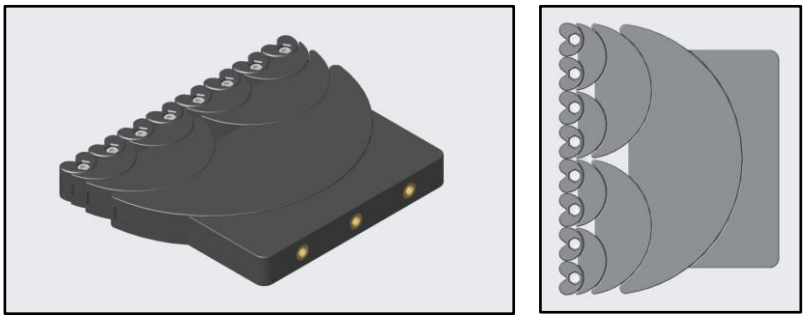

Picture 21. Isometric (left) and top (right) views of a Fractal Vise main components

The clamping jaws components in the Fractal Vise model below build up from a series of concentric arcs and a rectangular block as the side part connected to the vertical base plate of mounting interface. The semi-circular components are reduced by half-diameter to the next arcs in direction to the end of jaws teeth. From the figures below, the parts are categorized into four distinctive shapes: the first is a rectangular block with a single concave cutout; the second is a half-circle piece, referred to as Part C; the third is an arched profile with two concave cutouts, known as Part D; and the fourth is the eight part, which is symmetrical in both top and bottom views and functions as the clamping teeth [11]. At the final assembly model, two sub-assemblies of Fractal Vise are used in which each of them is placed at the horizontal base plates on the fixed-and move-able jaws of the Bench Vise.

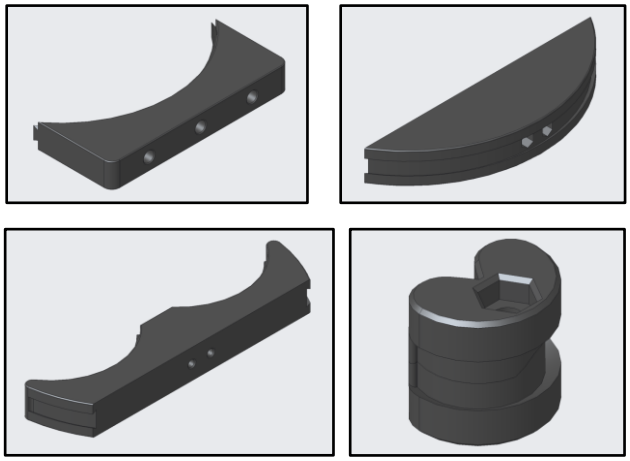

Picture 22. Isometric (left) and top (right) views of a Fractal Vise main components

An exploded view of the assembly (Picture 23) clearly illustrates how each fractal component, along with fasteners, bolts, nuts and threaded inserts, is arranged and interrelated. This visual breakdown makes the sequence of parts and their hierarchy much easier to understand and communicate.

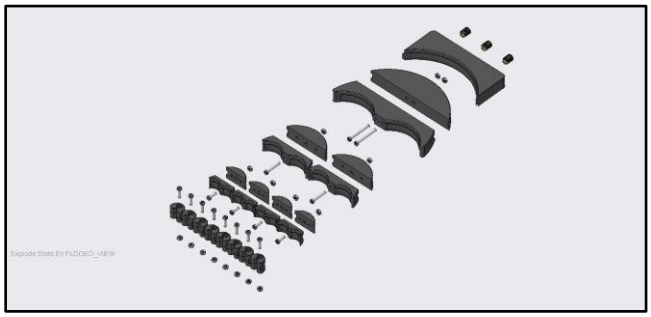

Picture 23. Exploded view model of the Fractal Vise assembly

Dovetail sliding mechanisms between Part 1 (male dovetail) and Part 2 (female dovetail) are designed as a clearance-fit system, specifically a running or sliding fir (RC-type) allowing guided motion with minimal play. In this configuration, the width of the male dovetail is 2.758 mm and the female grove is 1.918 mm. This intentional difference introduces a small clearance between the contact surfaces to allow Part 1 slides freely within Part 2 without jamming. Conversely, the height of the male dovetail (8 mm), should be slightly smaller than the female channel, which is *8.6 mm*, creating additional clearance at the vertical dimension to enable easy insertion from the open end.

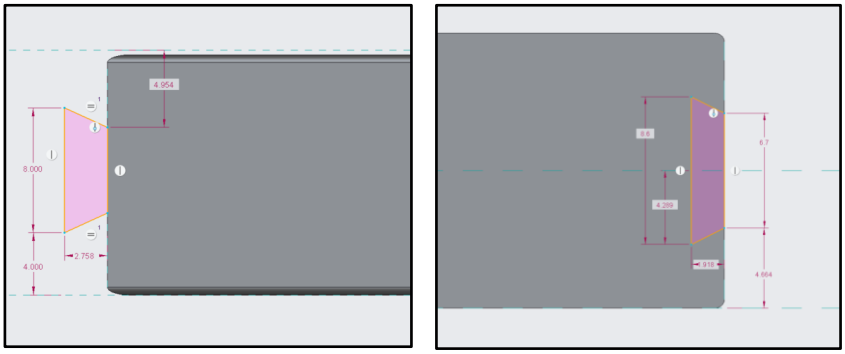

Picture 24. Dovetail dimensions of Part 1(left) and Part 2 (right)

The close-end dovetail track on Part D is designed to prevent the male dovetail of the previous Part D from sliding out during operation. While the Part C has only one female dovetail slot without a male feature, Part D includes both – a central male dovetail and female grooves on either side. The critical design detail is that the female grooves on Part D are at one end, effectively locking the preceding part in place. Because of this, the assembly must begin from the largest part from the right and progress sequentially to the left, thus each male dovetail fully engages before being secured by the closed-end grove of the next part [12].

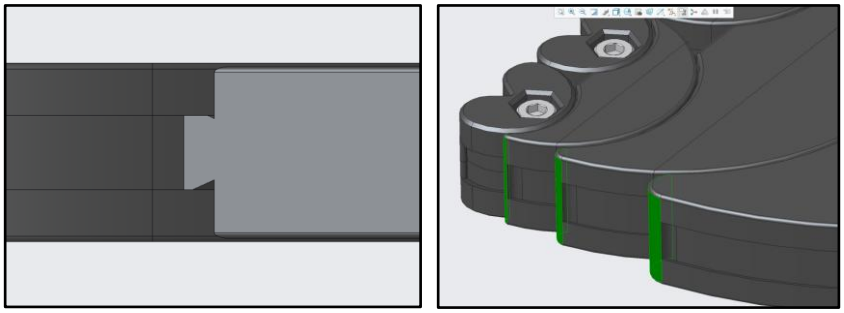

Picture 25. Dovetail insertion mechanism (left) and closed-end paths on female dovetails (right)

One of the parts that can be taken as an example of design process is Part 5, which serves as a Part D and contains two dovetail types. This part is initially sketched with a full circle of 70 mm diameter. The symmetric fractal shape was then constructed using arc-based cutouts, each with a *35 mm* diameter and centered along the same vertical centerline as the full circle. Unnecessary segments were removed using the *delete segment* feature to shape the double-lobed profile, with the flat back and front surface to accommodate mounting holes. The total length of the flat back surface was dimensioned at *60.32 mm*. with additional features like chamfers, rounds, and holes defined in later steps of model three to complete the component's structure.

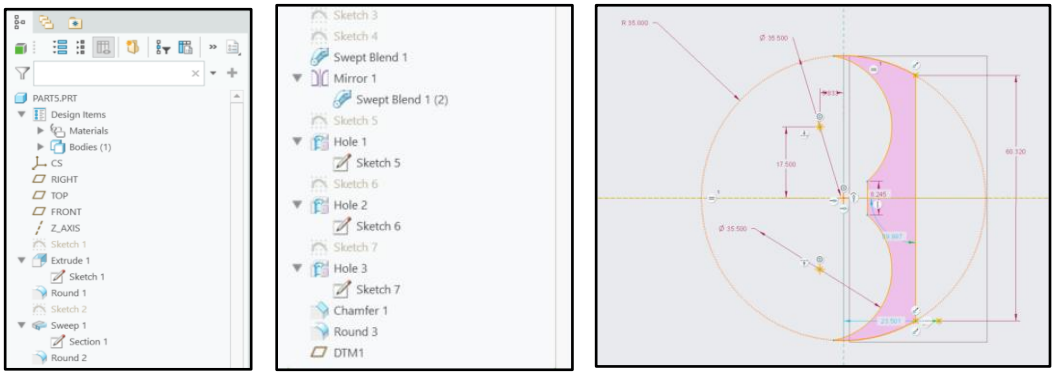

Picture 26. Design features and processes for Part 5

Following the main body, the sweep feature was applied to create the female dovetail grooves on each side by sketching the dovetail on one of the cutouts, requiring two identical end-section sketches and a connecting path to add material. This male dovetail was then mirrored to the opposite using the vertical midplane. The fourth step involved creating two types of holes: one central hole for an M3 bolt and hex nut, and two smaller holes (Ø2.2 mm, depth 5 mm) for filament insertion, placed on the flat back side. These small holes are essential where thermoplastic filaments will be inserted to prevent vertical degree of freedom of Part C (which has only one female dovetail).

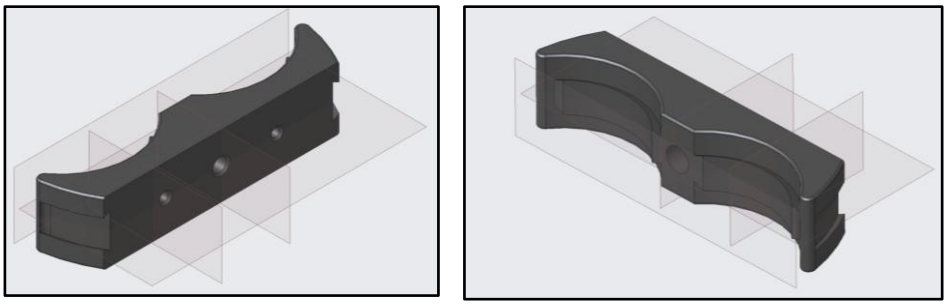

Picture 27. Isometric views of Part 5

Various sizes of fasteners and supporting inserts were applied in this assembly. The first image on the left illustrates how brass threaded inserts are embedded into the three holes on the back side of the first fractal component (Part 1), serving as the internal threads for M5x16 bolts during the final assembly with the mounting interface. The *Ø6.4 mm* diameter holes are intentionally smaller than the insert's outer diameter (Ø8 mm) to allow a proper interference fit once the inserts are heated and melted into the plastic material. The internal pitch diameter of the inserts is *Ø7.2 mm*. The middle figure shows the horizontal-axis connection between Part 4 (Part C) and Part 5 (Part D), fastened using an M3x20 bolt and M3 hex nut. Bolt lengths vary across the design – M3x10, M3x12, M3x20, M3x30 – depending on the position and parts involved. For instance, Part 8 in the right image uses vertical-axis fasteners (M3x12 bolts) to join two symmetrical clamping teeth components, with a total of 12 Part 8 units used per side of the Fractal Vise assembly.

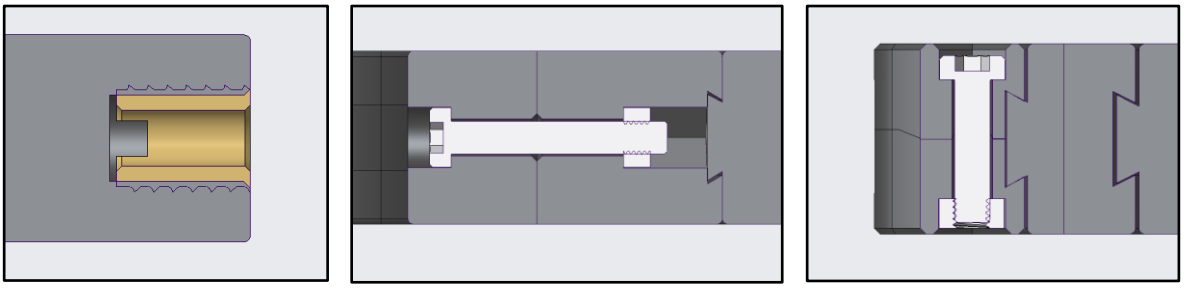

Picture 28. Threaded inserts, bolts, and nuts connections

The assembly drawing of the Fractal Vise below presents a combined half-view and half-section top view, which visualizes both the external appearance and internal structure. The left side shows the external geometry of fractal components, while the right-side sectioned half reveals the internal fastener assemblies, including bolts, hex nuts, and brass threaded inserts. The section view uses a plastic hatching pattern, indicating the primary material is *PETG-CF*, as noted in the title block. The overall dimensions of the assembly are *140 mm* in length, *113 mm* in width, and *16 mm* in height, with the base component (Part 1) measuring *112 mm* in length. An isometric view in the bottom left corner supports spatial understanding by showing the gradual scaling of fractal components. The bill of materials (BOM) lists 14 items, involving brass threaded inserts with three quantities, M3 hexagonal nuts with six quantities, and bolts in four different lengths. Item 7 to 14 represent structural and fractal parts, where Part 1 functions as the base and Part 8, used in the highest quantities (16 pieces), forms the smallest mirrored clamping teeth.

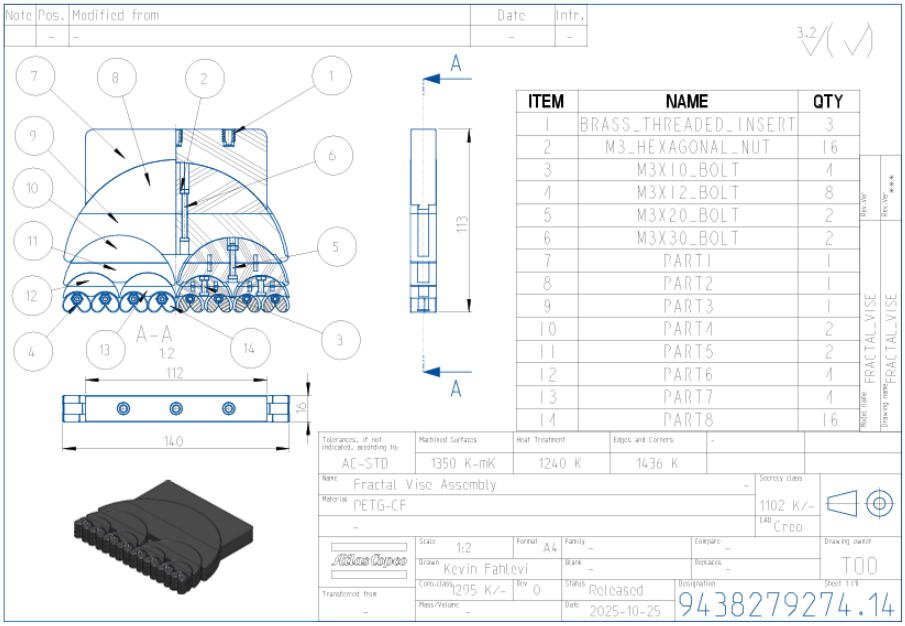

Picture 29. Assembly drawing of the Fractal Vise assembly

3.1.4 Bench Vise Assembly

The Bench Vise displays below served as the foundational structure in this project, equipping the primary frame and mechanical drive system for the integrated hybrid vise assembly. Made of cast steel, the vise is designed to ascertain high stiffness and durability during operation. Its robust body includes the fixed jaw and movable jaw system, operated via a lead screw, enabling rigorous linear movement for clamping tasks [13]. For this project, four M8X1.25 (STD) threaded holes were used as mounting points that allow the integration of the adaptive Fractal Vise system.

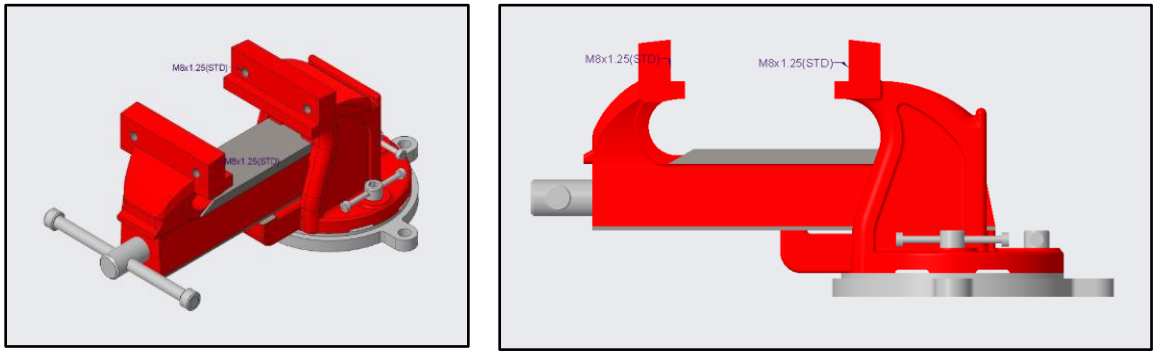

Picture 30. Isometric (left) and side (right) views of the Bench Vise model

The exploded view of the Bench Vise assembly below reveals its main components, starting from the fixed jaw base, movable jaw with embedded slide rail, and the rotating base discs which includes the lower and upper swivel plates. Here is also visible the M8X1.25 hex socket head screws, used to fasten the upper jaw assembly to the rear vertical frame, and the main lead screw with its associated handlebar and nuts for actuation. Four M6 bolts are shown at the top, likely for securing the base to a mounting surface or for locking the rotational base in place.

In the assembly process using PTC Creo, the model was built by applying various constraint types such as coincident, parallel, and distance to define spatial relationship accurately between parts. For instance, the sliding jaw was constrained along the linear axis using a distance mate, white the rotating base was aligned concentrically using coincident and axial constraints. This method ensures all components are assembled in their correct positions with realistic motion behavior and interference free connections.

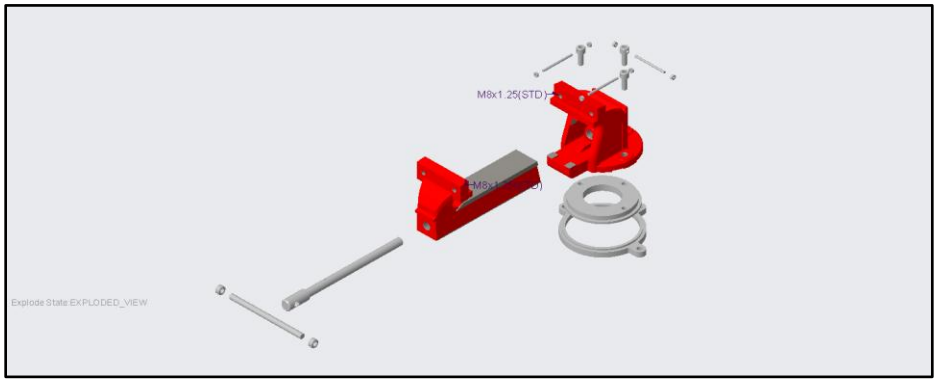

Picture 31. Exploded view model of the Bench Vise assembly

The technical drawing below illustrated the fully assembled Bench Vise model, detailing its important dimensions, structural components, and corresponding part numbers through balloon annotations. The assembly consists of ten key components, including jaw inserts, a sliding arm, fixed jaw inserts, a base plate, support, sliding block, main body, shaft, screws, and a small rod. Important dimensions are also specified: the base plate spans 180 mm in total width, with a mounting hole distance of 154 mm; the clamping width between the jaws reaches up to 135 mm, and the internal clamping depth is 38 mm. The overall height from the base to the top of the jaw measures approximately 141.3 mm. The base plate enables rotatable mounting, while the main body on the

right side serves as the central cast steel frame that supports all other components. The material used is EN 10293 G20Mn5 cast steel [14].

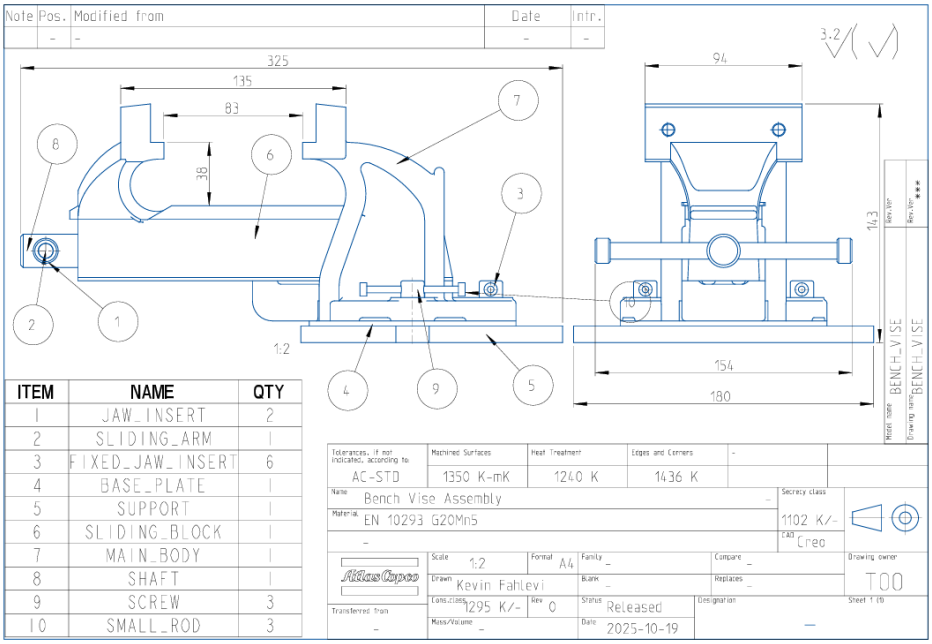

Picture 32. Assembly drawing of the Bench Vise assembly

3.2 MATERIAL SELECTION

Material choice profoundly impacts the performance and longevity of the vise assembly, particularly in key components such as the clamping jaws. For this application, material selection was based on criteria including mechanical strength, manufacturability, dimensional stability, and wear-resistance. Two sub-assemblies were targeted: the fractal clamping bodies and the mounting interface plates. The clamping components use a *PETG* intended for additive manufacturing, while the interface plates are made from *Aluminium 99.5* via subtractive manufacturing.

3.2.1 Carbon Fiber Reinforced PETG

PETG CF has been developed and implemented for a wide range of applications it requires a good balance between mechanical and optical material properties. The raw material is certified according to official standardization: REACH (Registration, Evaluation, Authorization, and Re-

striction of Chemicals) and RoHS (Restrictions of Hazardous Substances) [15]. This type of thermoplastic polymer is reinforced with carbon fibres, but it preserves its natural characteristics as a thermoplastic in a way that it can be repeatedly softened by heating and then solidified by cooling.

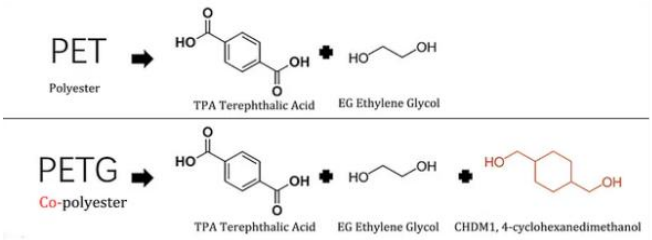

Picture 33. Difference between PET and PETG in terms of chemical structures

Polyethylene terephthalate glycol (PETG) is a modified form of Polyethylene terephthalate (PET), which both belong to the thermoplastic polyester family. PET itself is produced through the polymerization of terephthalic acid (TPA) and ethylene glycol (EG), forming a semi-crystalline structure with great strength but low grade in flexibility and processability. PETG is then produced to tackle these limitations by integrating an extra monomer, 1,4-cyclohexanedimethanol (CHDM), which raises its amorphous volume and enhances its ductility, transparency, and ease of thermal processing [16].

When carbon fibers are added into PETG, the composite gains significantly improved stiffness, tensile strength, and dimensional stability, at the same time still preserving good printability and layer adhesion and reducing deformation under mechanical load. This explains why PETG – CF is an ideal choice for functional prototypes and medium-duty structural components for work holding devices such as the clamping jaws of a Fractal Vise.

Picture 34. Bambu Lab's PETG - CF filament

The mechanical properties of PETG – CF exhibit notable anisotropy, with superior performance in the X-Y direction due to printing orientation. According to Bambu Lab, Young's modulus for the PET CF is around *2460 ± 230 MPa* in the print X-Y plane (about double of normal PETG) and around *1340 ± 150 MPa MPa* through the layer (Z axis). The range of ultimate tensile strength is roughly *35 MPa ± 5 MPa* (XY) and *29 ± 4 MPa* (Z) in that material. In fact, carbon fibre reinforcement can triple the tensile modulus of PETG and approximately double its strength compared to the unfilled polymer (at the cost of reduced elongation) [17]. The bending strength reaches *70 ± 5 MPa* (X-Y) and *48 ± 4 MPa* (Z). Elongation at break is low in the Z direction (4.7 ± 0.4%), showing reduced ductility along the build axis. Impact strength is good, especially in the X-Y direction (41.2 ± 2.6 kJ/m² unnotched), indicating toughness against sudden loads.

Mechanical Properties		
Subjects	**Testing Methods**	**Data**
Young's Modulus (X-Y)	ISO 527, GB/T 1040	2460 ± 230 MPa
Young's Modulus (Z)	ISO 527, GB/T 1040	1340 ± 150 MPa
Tensile Strength (X-Y)	ISO 527, GB/T 1040	35 ± 5 MPa
Tensile Strength (Z)	ISO 527, GB/T 1040	29 ± 4 MPa
Breaking Elongation Rate (X-Y)	ISO 527, GB/T 1040	10.4 ± 0.6 %
Breaking Elongation Rate (Z)	ISO 527, GB/T 1040	4.7 ± 0.4 %
Bending Modulus (X-Y)	ISO 178, GB/T 9341	2910 ± 260 MPa
Bending Modulus (Z)	ISO 178, GB/T 9341	1560 ± 180 MPa
Bending Strength (X-Y)	ISO 178, GB/T 9341	70 ± 5 MPa
Bending Strength (Z)	ISO 178, GB/T 9341	48 ± 4 MPa
Impact Strength (X-Y)	ISO 179, GB/T 1043	41.2 ± 2.6 kJ/m²; 15.7 ±1.6 kJ/m² (notched)
Impact Strength (Z)	ISO 179, GB/T 1043	10.7 ± 1.6 kJ/m²

Picture 35. Mechanical properties of PETG – CF

Due to anisotropy and layer dependence, a 2x safety factor is advised for *PETG - CF* in load bearing roles. For instance, if a part experiences *100 N*, test it for *>200 N.* Typical working stress should stray around *15 – 20 MPa* (given *30 – 50 MPa* ultimate strength). Align major stresses with the fibre-filled X-Y plane for maximum strength and avoid Z-axis loading in critical paths [18].

3.2.2 Aluminium 99.5

Delivery condition[5]	Nominal thickness mm		Tensile strength R_m MPa		Elastic limit $R_{p0.2}$ MPa		Elongation % min.		Bending radius[9]		Hardness[9] HBW
	over	to	min.	max.	min.	max.	A50 mm	A	180°	90°	
H14	0,2	0,5	105	145	85	-	2	-	1,0 t	0 t	34
	0,5	1,5	105	145	85	-	2	-	1,0 t	0,5 t	34
	1,5	3,0	105	145	85	-	4	-	1,0 t	1,0 t	34
	3,0	6,0	105	145	85	-	5	-	-	1,5 t	34
	6,0	12,5	105	145	85	-	6	-	-	2,5 t	34
	12,5	25,0	105	145	85	-	-	6	-	-	34
H24	0,2	0,5	105	145	75	-	3	-	1,0 t	0 t	33
	0,5	1,5	105	145	75	-	4	-	1,0 t	0,5 t	33
	1,5	3,0	105	145	75	-	5	-	1,0 t	1,0 t	33
	3,0	6,0	105	145	75	-	8	-	1,5 t	1,5 t	33
	6,0	12,5	105	145	75	-	8	-	-	2,5 t	33
O / H111	0,2	0,5	65	95	20	-	20	-	0 t	0 t	20
	0,5	1,5	65	95	20	-	22	-	0 t	0 t	20
	1,5	3,0	65	95	20	-	26	-	0 t	0 t	20
	3,0	6,0	65	95	20	-	29	-	0,5 t	0,5 t	20
	6,0	12,5	65	95	20	-	35	-	1,0 t	1,0 t	20
	12,5	80,0	65	95	20	-	-	32	-	-	20
H112	≥ 6,0	12,5	75	-	30	-	20	-	-	-	23
	12,5	80,0	70	-	25	-	-	20	-	-	22
5	*Other possible delivery conditions for this alloy: H12 · H16 · H18 · H19 · H22 · H26 · H28*										
9	*For information only*										

Picture 36. Mechanical strengths of Aluminum 99.5 sheet/plates

Aluminum 995% (EN AW 1050A) is a high-purity, non-heat-treatable alloy known for its corrosion resistance, high electrical and thermal conductivity, and good formability. It contains at least 99.5% aluminum with small traces of Fe (≤0.4%), Si (≤0.25%), and others (≤0.05%) [19].

In the O (annealed) temper, it is soft and ductile with *65–95 MPa* tensile strength, *20 MPa* yield strength, and 20–35% elongation. The H14 (half-hard) condition offers a balance of strength and formability, with *105–145 MPa* tensile and *85 MPa* yield strength, but only 2–6% elongation. The H24 (strain-hardened) temper provides *105–145 MPa* tensile and up to *75 MPa* yield strength, with 3–8% elongation. Hardness ranges 20–34 HBW. The H18 temper gives maximum strength and minimum ductility [20].

Specifications in % Remainder: Aluminium												Other	
Si	Fe	Cu	Mn	Mg	Cr	Ni	Zn	Ti	Ga	V	Note	Individual	Total[2]
0,25	0,40	0,05	0,05	0,05	-	-	0,07	0,05	-	-	-	0,03	-
X	*Chemical specifications as perc. of weight. If no ranges are specified, the alloy content has the maximum value.*												
2	*Includes all items listed for which no limit values are specified.*												

Picture 37. Chemical composition of Aluminum 99.5

Al 99.5 is easy to shape, cut, stamp, and machine due to its high ductility and purity. Alloy 1050/1100 is often used for deep drawing or spinning because of its excellent formability. Machining pure aluminum is simple but can cause built-up edges if cut too slowly or without lubrication. It machines best when cold-worked (**H14/H18**) using carbide tools. In the soft state, it may stick to cutters, so sharp tools, high speeds, and proper cutting fluids are recommended. Pure aluminum is less free machining than alloys like 6061 or 2011 since it lacks silicon and other impurities. Still, 99.5% Al performs well in CNC milling or drilling, though swarf can be more persistent. When tapping threads, care is needed to prevent galling or shearing if thread engagement is too shallow.

Picture 38. Aluminum 99.5 plate/sheet

3.3 MANUFACTURING PROCESSES

The manufacturing processes selected for this project, particularly for the Fractal Vise components and mounting interface base plates, were based on the distinct functional requirements and material characteristics of each component. As 3D printers with the brand from Bambu Lab are facilitated at Atlas Copco Hungary, additive manufacturing using *PETG – CF* was chosen for producing the complex fractal structures due to its flexibility in fabricating intricate geometries, reduced material waste, and suitability for prototyping with reinforced thermoplastics. Meanwhile, subtractive manufacturing through CNC milling was applied to machine the Aluminum 99.5 parts, for the mounting interfaces, where dimensional accuracy especially for holes, surface finish, and mechanical rigidity are critical.

3.3.1 3D Printing

At Atlas Copco Hungary, the *Bambu Lab X1 Carbon* 3D printer is utilized for fabricating functional thermoplastic parts which made for the production line and manufacturing shopfloor, including those made from *PETG – CF* filament. This advanced printer is equipped with a *0.4 mm*

nozzle, offers an optimal balance or moderate to high strength between printing speed, surface resolution, and structural integrity. While *0.2 mm* nozzles provide finer detail and *0.6 – 0.8 mm* nozzles deliver faster, stronger prints with rougher surfaces, so overall the *0.4 mm* size is best suited for functional prototyping and tooling needs the company, especially to manufacture this product [21].

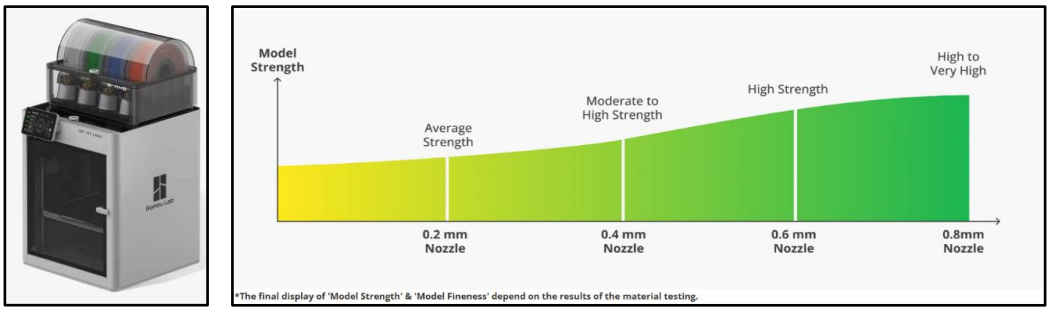

Picture 39. Bambu Lab X1 printer (left) and comparison of different nozzle-types (right)

After being discussed among engineer pears at Atlas Copco Hungary that selected material for the fractal parts is *PETG – CF*, the development process followed by 3D printing software configurations which involve several precise settings. A total of 20 individual parts is placed on the digital printing board with the automatic and optimized placement orientation; all parts are oriented with their flattest surface against the textured PEI plate, which improves bed adhesion and minimizes the risk of warping or detachment during printing. The other arrangements such as 2 large, curved clamps at the rear of the plate, 6 medium clamps in two rows of three, and 12 small parts are tightly grouped in the front of the plate, arranged in a grid pattern are to support the space utilization and print efficiency while avoiding collision. This setup also allows the printer to reduce travel time between parts.

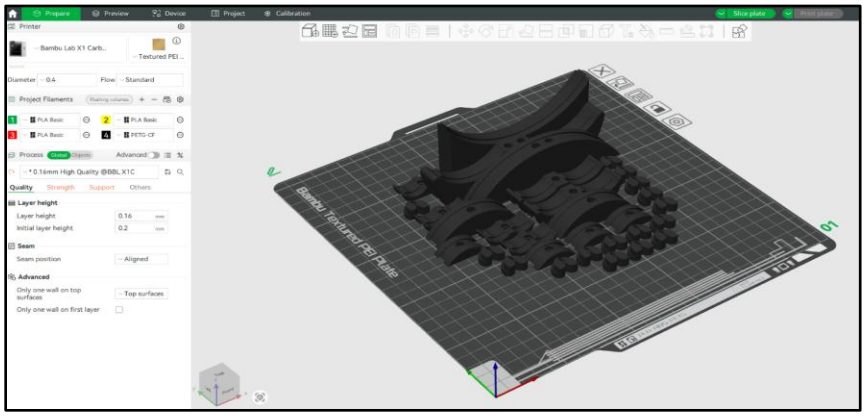

Picture 40. 3D printing layout of Bambu Lab X1 (Quality tab)

Under *Quality*, the layer height is *0.16 mm* for high resolution, with an initial layer of *0.2 mm* for better adhesion. The seam is aligned to a cleaner top surface. Under *Strength*, wall loops are 5, with 6 top and 4 bottom layers using a monotonic pattern for smoother finish. A 50% gyroid infill density provides a balance of strength and material use. Under *Support*, automatic supports with a 25° threshold are limited to the build plate to minimize material waste.

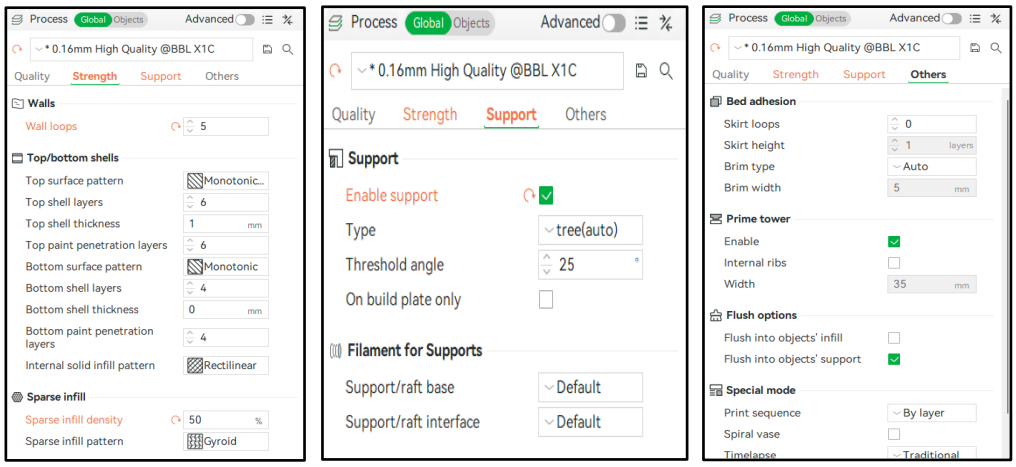

Picture 41. 3D printing configurations (Strength, Support, and Others tabs)

When it comes to the slicing process, the model requires 192.33 g of total filament, with 191.7 g used for the parts and 0.63 g for supports, without any filament change during the process. The estimated print time is 13 hours and 28 minutes, with a total time of 13 hours and 37 minutes including an 8-minute preparation phase. Most time is spent on sparse infill (36.3%) and inner walls (28.4%), followed by outer walls and internal solid infill. The chosen *0.4 mm* nozzle operates across various speeds, from *8 mm/s* for precise movements up to *250 mm/s* for rapid travel paths. These slicing parameters were carefully configured to balance strength, detail, and efficiency for functional mechanical components.

Picture 42. Time estimation and speed variations during slicing

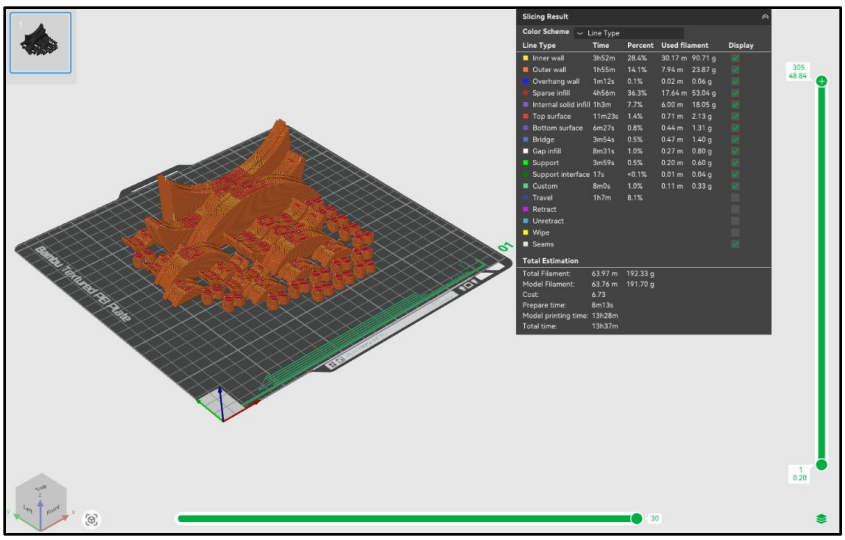

Picture 43. Slicing results of fractal components

After completing the configuration in the *Bambu Studio software*, the selected PETG – CF filament was loaded into the AMS (Automatic Material System), and the *Bambu Lab X1 Carbon* 3D printer was prepared for operation. The printer setup included temperature calibration, bed levelling, and final confirmation of slicing parameters. As shown in the picture below, the machine interface displayed the initial printing process. However, at this stage, only a short 1 hour 57-minute print was conducted to produced 2-3 sample parts. This preliminary run served as a test to verify adhesion, support generation, wall quality, and overall compatibility of the slicing settings before proceeding to the full-scale production of the complete batch.

Picture 44. 3D printing for the sample fractal components

3.3.2 Milling and Drilling

Parallel to the additive manufacturing processes of the fractal components, the designed mounting interface plates are also continued to the manufacturing stage, after *Aluminum 99.5* was used as a base material. Two subtractive manufacturing machines are utilized at Atlas Copco Hungary, where each of them used for milling and drilling purposes. The first machine, *INTOS FNGJ 40*, is manufactured by INTOS spol. s.r.o. is a universal toll-room milling machine designed for vertical and horizontal milling operations. It features a swiveling vertical spindle head, a tilting ram, an *800 x 400 mm* working table, additionally supported by the stepless spindle speeds by means of frequency converter in 2 steps, with max *4000 RPM* [22].

The machine is equipped with hardened guideways for long-term durability, central lubrication via dosing devices for smooth operation, and hand wheels with fine 0.01 mm divisions in X, Y, and Z axes for precise manual positioning. Cooling systems are integrated, although the standard execution uses manual tool clamping, optional upgrades allow for pneumatic-hydraulic tool clamping in both vertical and horizontal spindles. With its compact layout, oil resistant surface paint, and reliable electrical system (3x400V, 50 Hz), this machine is appropriate for a standard application at the maintenance or manufacturing shopfloor.

Picture 45. Milling machine FNGJ 40 used for milling processes

The second machine, the Bridgeport Series I, is a precision knee-type vertical milling machine by Bridgeport (Hardinge Inc.). It has a 9”×49” (229×1245 mm) worktable with travels of 36” (X), 12” (Y), and 16” (Z), plus a quill travel of 5” (127 mm) for fine depth control. Driven by a 2 HP continuous motor (3 HP peak), the spindle runs between *60–500 RPM* and *500–4200 RPM*, suitable for various drilling and light milling tasks. It uses an R-8 taper, manual handwheels with *0.01 mm* precision, hardened guideways, one-shot lubrication, and a cast-iron body for stability.

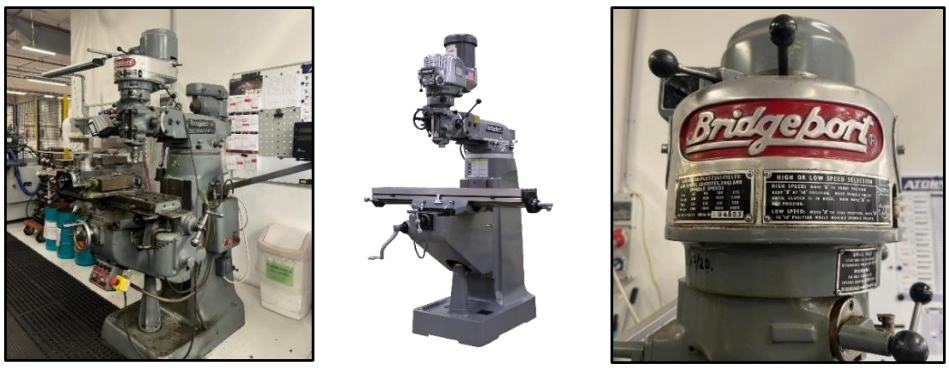

Picture 46. Milling machine Bridgeport Series I used for drilling processes

The initial milling processes involved a collection of milling tools utilized with the *FNGJ 40* to accurately shape Aluminium base plates to their required dimensions. These tools as displayed in the Picture 40 (left), are mounted in standardized tool holders; among them are likely face mills for the flat surfaces over large areas, end mills which perform contouring pocketing, and slotting operations, and chamfer or shell mills for edge finishing and bulk material removal. With the ability of X, Y, Z-axis movement, the maintenance operator at Atlas Copco was able to conduct rough and fine milling tasks efficiently across the entire workpiece [23].

Following the milling stage, the prepared plates were transferred to the *Bridgeport Series I*. The drilling process began with a centre drill to precisely locate the hole position, followed by a *Ø4.2 mm* drill bit for M5 tapping holes and a *Ø5.2 mm* drill for a through-hole. A countersink tool was then used to create a chamfer at the hole entrance, easing the threading process with hand taps for both M5 and M8 threads. Lastly, another chamfering operation was applied to smooth both ends of the threaded holes.

Picture 47. Collection of milling (left) and drilling (right) tools used for the mounting interface plates – left to right order

4. RESULTS AND DISCUSSIONS

4.1 Assembling and Prototyping

This sub-chapter details the development stage of the Fractal Vise system, assembly of manufactured base plates, focusing on prototyping of each unit. During prototyping, all individually machined components of the Fractal segments and mounting interface base plates are carefully assembled to the Bench Vise, to form the complete hybrid system and assess its applicability. The goal of this chapter is to evaluate the accuracy of fabrication, fitment of parts, and structural alignment.

4.1.1 Prototyping of Fractal Vise

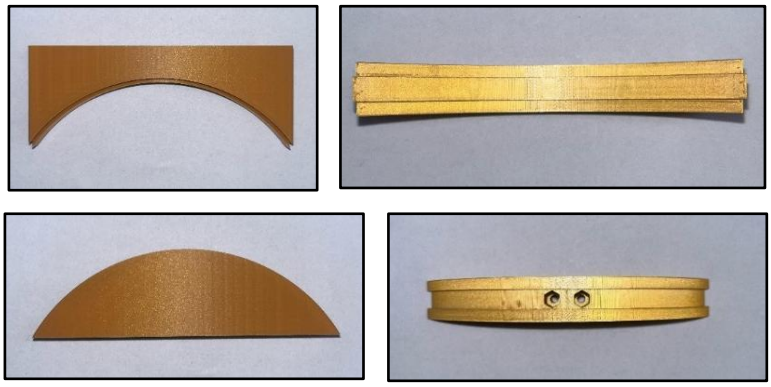

Picture 48. Sample Part 1 (top) and Part 2 (down) - top and front views

To begin prototyping the Fractal Vise, two main parts were produced to test dimensional alignment and fitness, focusing on the dovetail connection. The first part includes a c-shaped dovetail slot and two central holes for M3 hex nuts and bolts. During assembly, bolts are inserted and unscrewed to lock the nuts in place, after which the second component, designed to slide into the dovetail track, is guided into position.

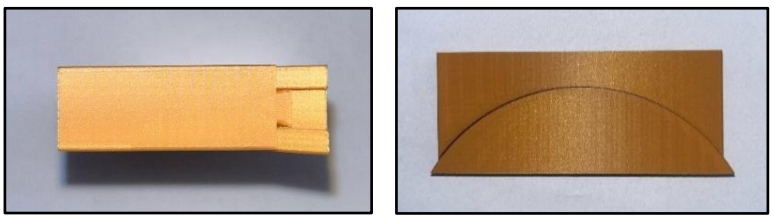

Picture 50. Assembled sample parts of Fractal vise – side (left) and top (right) views

The eight individual components of the Fractal Vise assembly are shown below, each with top views, arranged sequentially from top to bottom as Part 1 through Part 8. On the back side of Part 1, three simple flat holes are created with diameter *Ø6.4 mm* and depth *10.5 mm* which are aligning to the holes of vertical base plate of mounting interface. Part 2 features two holes, while the remaining parts have a single hole of *Ø3.4 mm* with various depths, smaller shape leads to shorter depths. All parts are connected horizontally with M3 bolt and hex nuts, except for the last two components (part 8) which are vertically connected through similar fasteners. Furthermore, each part C (part 2, 4, and 6) contains two tiny side holes to insert *1.76 mm* filament sections, which help secure part C and part D together during assembly [24].

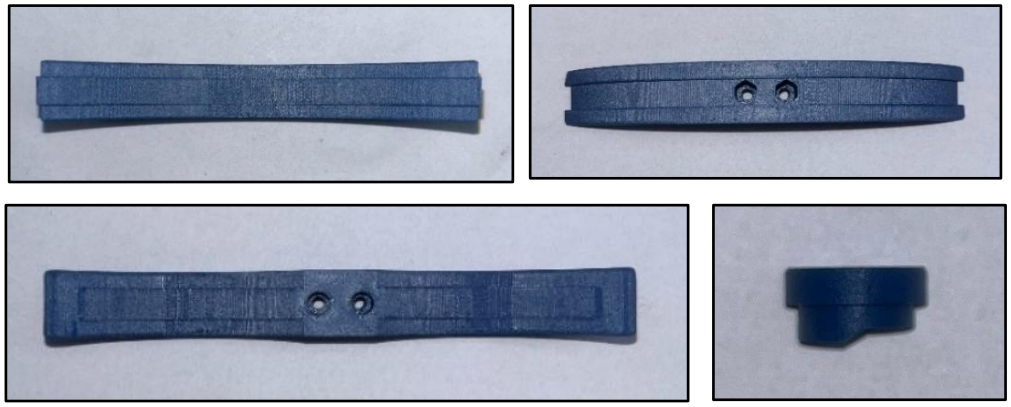

Picture 51. 3D printed Part 1, Part C, Part D, and Part 8

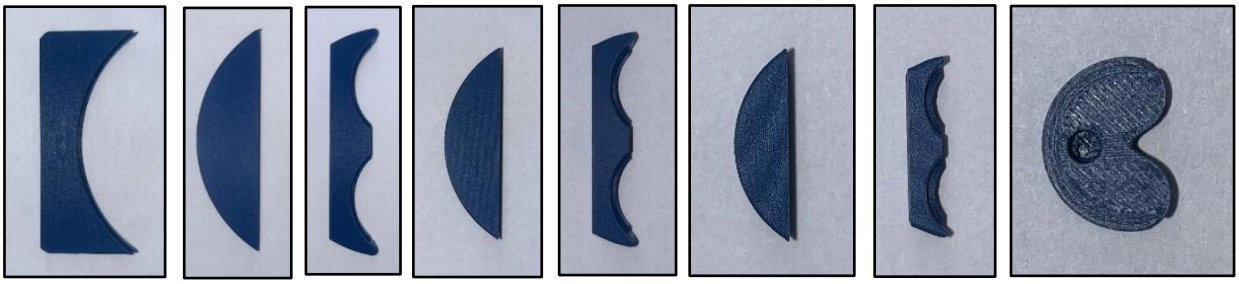

Picture 52. Eight parts of Fractal Vise components – front Part 1 (left) to Part 8 (right)

Following the earlier assembly steps, the half-assembled Fractal Vise was secured in a Bench Vise to stabilize the position while continuing the prototyping of the remaining-half processes. The next stage involved the insertion of M3 bolts and nuts into the designated holes on each part using a manual screwdriver. To reinforce the connection between part C (semi-circular) and part D (arc with dual cutouts), *Loctite* adhesive was carefully applied near the small filament

pinholes. This provided additional bonding strength around the interface. Subsequently, to enhance rotational movement along the dovetail tracks, the mating surfaces of each part were deburred with a small file, followed by the application of grease to reduce friction. The parts were then moved back and forth to evenly distributing the lubricant and assessing the smoothness and precision of the sliding fit.

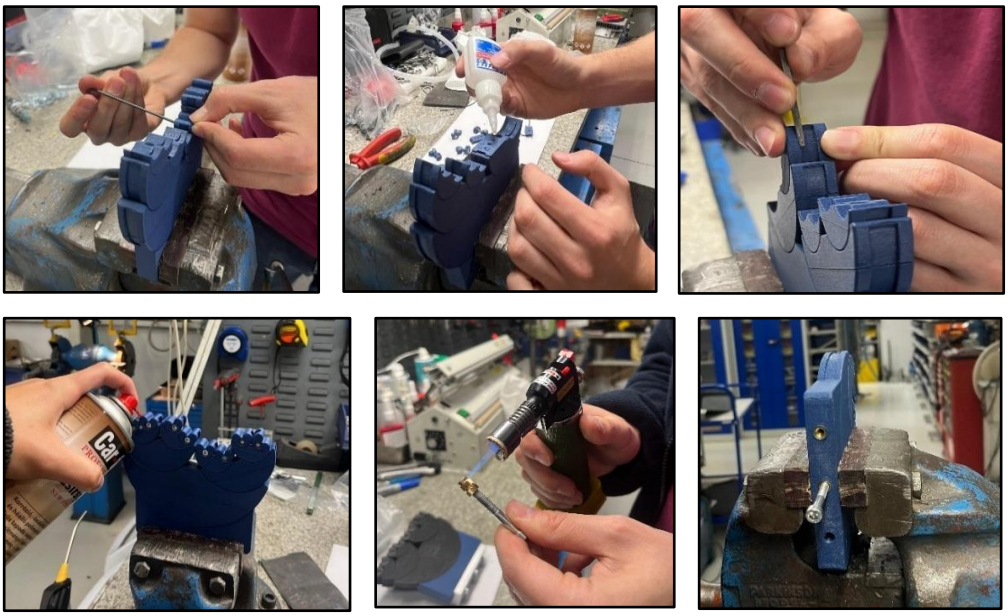

Picture 53. Assembling and prototyping processes of Fractal Vise

The final step shown above involved preparing the first part to accept the threaded brass inserts. These inserts were heated using a soldering iron to slightly melt the plastic and allow precise insertion into the three holes on the back side of the component. Once cooled, the inserts provided durable threads to accommodate bolt connections with the mounting interface plate. The final assemblies of the Fractal Vise as displays below showcase the successful integration of all eight 3D-printed parts, which reflects a complete prototyping process involving part validation, manual assembly, lubrication, adhesive bonding, and heat-set threaded inserts process.

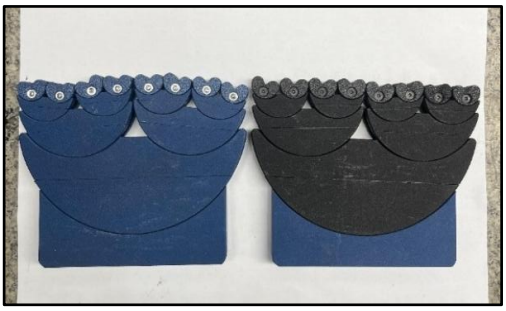

Picture 54. Final prototyping results of Fractal Vise assemblies

4.1.2 Prototyping of Mounting Interface

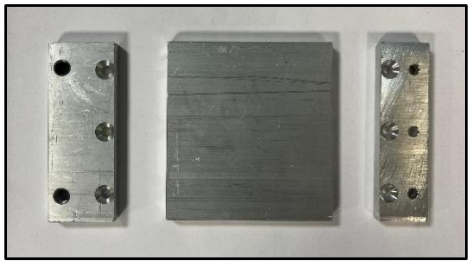

Picture 55. Original base plates of mounting interface

The prototyping process of the mounting interface began by modelling and fabricating three *Aluminium* base plates using milling and drilling machines, as elaborated in the previous chapter. The picture above shows three original base plates including two vertical plates and one horizontal plate as a main landing space for the Fractal Vise, built with the same width. The picture below displays the plates were machined with *Ø5.2 mm* simple-drilled and countersink holes to accommodate M5 screws for secure assembly of two connection points. After machining, the components were assembled manually using a screwdriver to fasten sic screws.

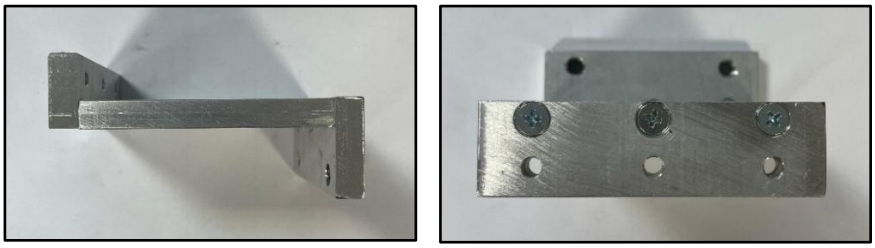

Picture 56. Assembled original parts of base plates - side (left) and front (right) views

In the improvement stage, the mounting interface was upgraded by increasing the base plates from three to four. A new horizontal base plate was added to partially cover the Fractal Vise, and the third plate was redesigned with six countersink and three drilled holes, aligned with the first part's backside holes. The final setup shows the complete mounting interface, each supporting one Fractal Vise unit.

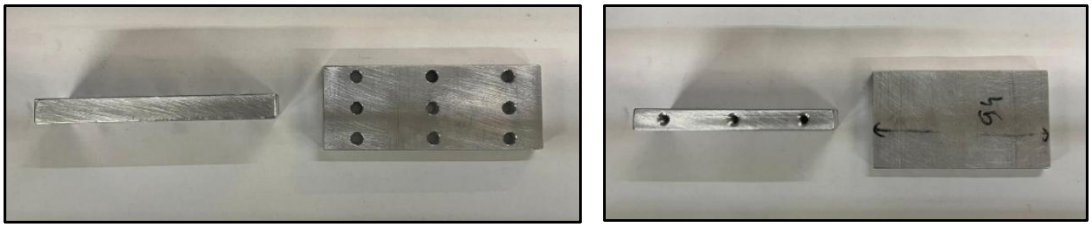

Picture 57. Improved (left) and additional (right) base plates of mounting interface

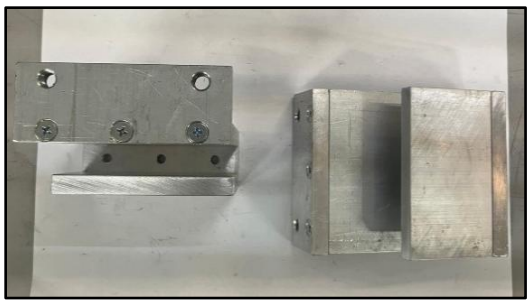

Picture 58. Final prototyping results of mounting interface assemblies

4.1.3 Final Integration of Prototype Systems

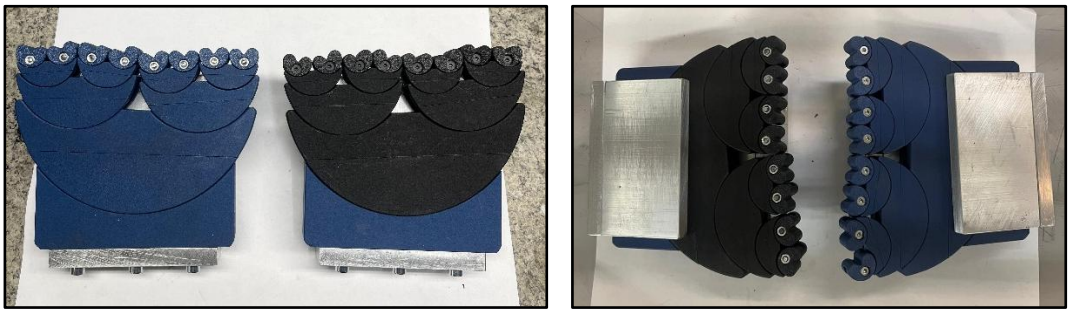

Picture 59. Top views of the Fractal Vise and mounting interface assemblies - original (left) and upgraded (right) versions

The top-left image presents the integration of the Fractal Vise with the original mounting interface, while the top-right image shows the upgraded version, where an additional horizontal plate has been introduced to partially cover (52 mm) the top of the Fractal Vise; provides enhanced stability and enclosure. In both versions, the primary connection between the Fractal Vise and the mounting interface occurs through the third vertical base plate, which aligns with three threaded-insert holes on the back side of the vise using M5X20 bolts. The bottom image captures the front view of both fully assembled Fractal Vise units with the improved mounting interface.

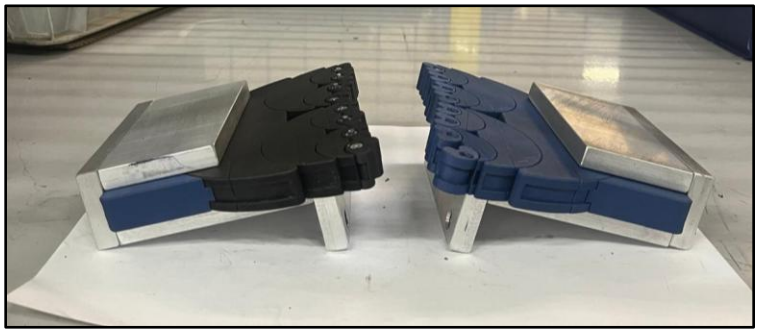

Picture 60. Front view of the Fractal Vise and upgraded mounting interface assembly

There are several workshop tools utilized for the final integration process, as displays in the image below (left). Four M8x30 bolts were applied to fasten the mounting interfaces securely onto the vise jaws. Two screwdrivers were employed: the white-handled one was used to remove the original jaws of the Bench Vise, while the red-and-black driver, with its longer shaft, was specifically chosen to insert and tighten the M8 bolts without interference from the horizontal base plate. The right image below shows the actual installation process using these tools.

Picture 61. Installation tools (left) and the prepared Bench Vise (right)

Following the successful installation of the Fractal Vise components and mounting interface plates onto the Bench Vise, the fully assembled setup was ready for functional evaluation. The next phase involved experimental testing, with a variety of industrial workpieces of different cross-sectional geometries, aimed at assessing the adaptability, grip strength, and overall clamping performance of the system. As shown in the Picture 62, the initial configuration demonstrated the first stage development but revealed some limitations in structural stability during the testing operations. To address this, an upgraded version incorporating additional cap plates was modelled to reinforce the orientation, as depicted in the Picture. This enhancement significantly improved steadiness and structural balance of both fractal components and clamped workpiece, to be in the same straight line of working axis.

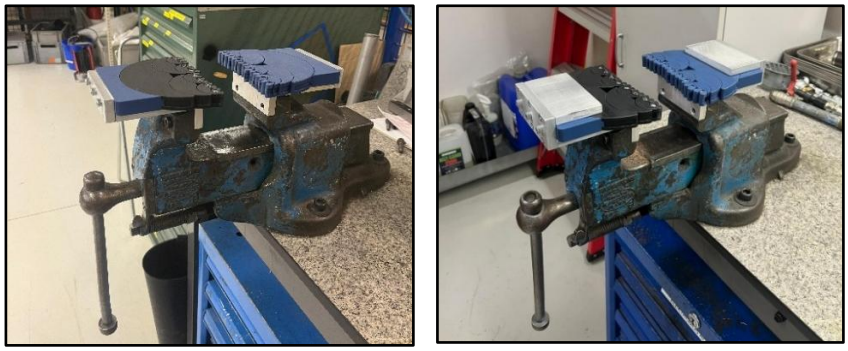

Picture 62. First model (left) and second model (right) of the vise integration assemblies

4.2 Experimental Testing

The experimental testing examined the vise assembly's performance under realistic workshop conditions, focusing on clamping strength, stability, and usability. The first model, without the cap plate, was tested using three workpieces - a cutting plier, socket wrench handle, and ratchet torque wrench. During testing, all clamping teeth (Part 8) were observed to move and adapt individually to the workpiece surface as torque was applied on the Bench Vise handle. This torque generated linear force across the fractal components, allowing the clamping system to adjust dynamically. In observations, the vise modified symmetrically to match the convex geometry of certain tools, where both sides mirrored each other. In contrast, for more complex shapes like the socket wrench handle, it showed asymmetrical adaptation - the blue side aligned with the straight shaft while the black side adjusted to the wider wrench head.

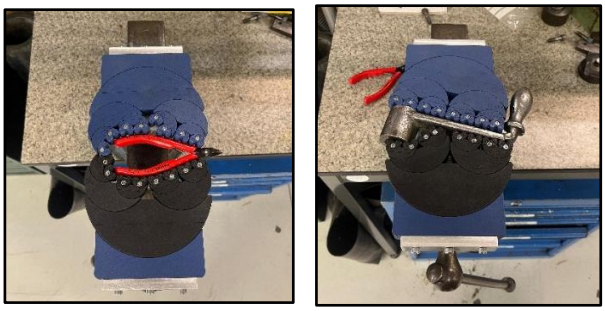

Picture 63. First model of Fractal Vise testing on cutting plier (left) and socket wrench handle (right) – top views

The clamping test was extended to a larger tool, a *420 mm* ratchet torque wrench, while the Fractal Vise front covered about one-third of its length - exceeding the vise's own size. Despite this scale difference, both the black and blue teeth are symmetrically adjusted to grip the wrench's curved head, proving this typical vise system is also work with large-shaped tools.

Picture 64. Fractal Vise testing on large tool (ratchet torque wrench) - isometric view

During further testing of the Fractal Vise, a mechanical limitation was observed, as shown in the images below. In the left picture, when clamping a workpiece, the blue side (left body) displays a noticeable upward bending near the bottom section, whereas the black side (right body) remains aligned with the horizontal plane of the mounting plate (Part 2). The deformation on the blue side begins at Part 2 and visibly affects the left portion of the entire vise. The bending deviation appears to be approximately 2.5 mm to 3 mm at its peak, particularly on the lower edge. From a mechanical perspective, this asymmetric deformation occurs because the blue side is connected to the fixed jaw of the Vise, which is subjected to reaction forces when clamping pressure is applied. On the other hand, the black side is supported by the moving jaw, which travels to apply pressure but is not structurally restrained which push freely without resistance. This means the fixed side must absorb both the clamping reaction force and potential torsional moments from the shifting load, leading to upward flexing if the material lacks sufficient stiffness. The right image reveals this bending effect in closer view: the horizontal alignment is disrupted, and the blue body tilts upward due to local deflection under concentrated stress.

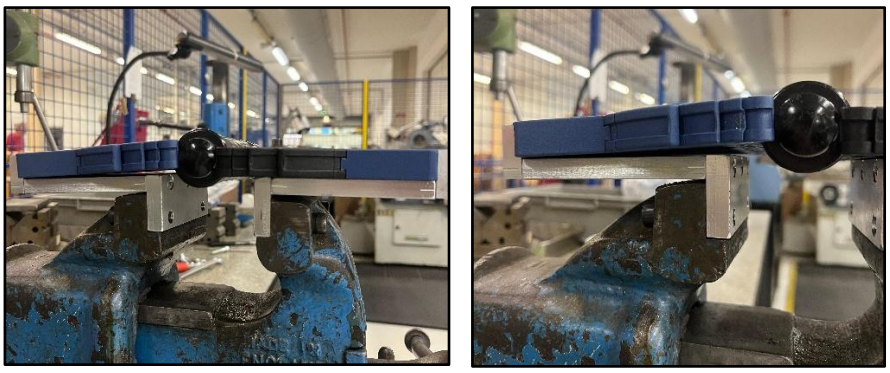

Picture 65. Observed bending during the application trial of first model – side views

Following the previous observation of bending deformation in the initial vise integration model, a second stage of experimental testing was conducted using an upgraded version that includes an additional cap plate. Five different tools were tested, arranged from simplest (left) to most complex (right) in shape; a rectangular steel block, a quick-release hydraulic connector, a 13 mm wrench, a water hose connector (with a brass thread and plastic nozzle), and a heavy-duty ball valve. In each case, the clamping teeth of the Fractal Vise automatically adjusted to match the varying geometries of the objestcs. For instance, the wrench and valve were clamped effectively, where symmetrical

adjustment of both clamping sides were created and independently secure contact with their surfaces.

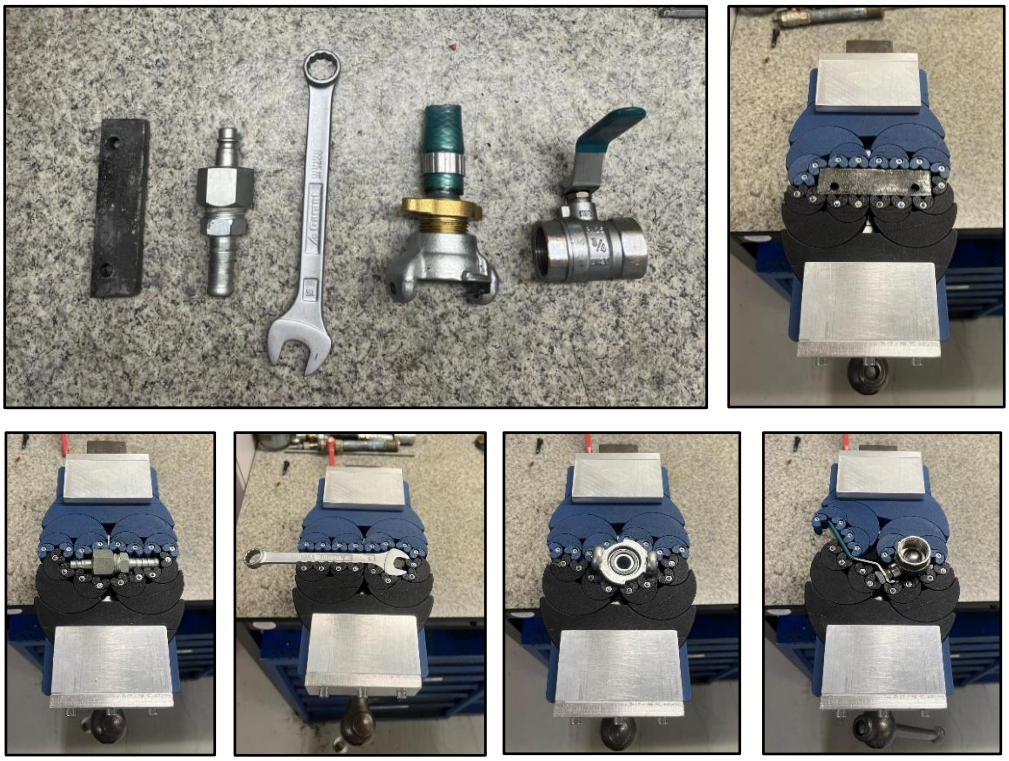

Picture 66. Second model of Fractal Vise testing on five different tools – top views

The side view photographs of this improved assembly display a major advancement in structural stability. By integrating a cap plate that spans half of the vise length – especially covering the dovetail section of Part 2, where the previous flexural bending occurred – the deformation issue was reduced. Under the same amount of applied torque to the Bench Vise, both sides of fractal assembly remained aligned with the horizontal mounting plate and did not exhibit the upward deflection see in the earlier model. From a mechanical standpoint, this improvement can be attributed to the increased second moment of area (moment of inertia), which governs flexural stiffness. Since the second moment of area, *I* for a rectangular cross-section is proportional to the cube of its height h ($I = 12bh^3$), even a small increase in height leads to a substantial increase in stiffness. Compared to the original configuration without the cap, the addition of a 10 mm-tall cap over a 52 mm span results in an approximate increase in bending stiffness by up to 300-4005 in the reinforced region. This effectively redistributes the clamping stress across a larger area and restrains

vertical deflection, thereby eliminating the initial flexural failure seen at the unreinforced first model.

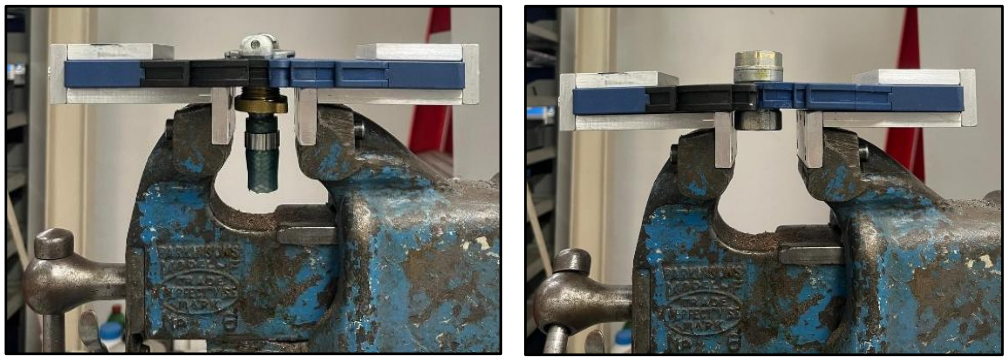

Picture 67. Second model of Fractal Vise testing on water hose connector (left) and ball valve (right) - side views

4.3 Finite Element Analysis

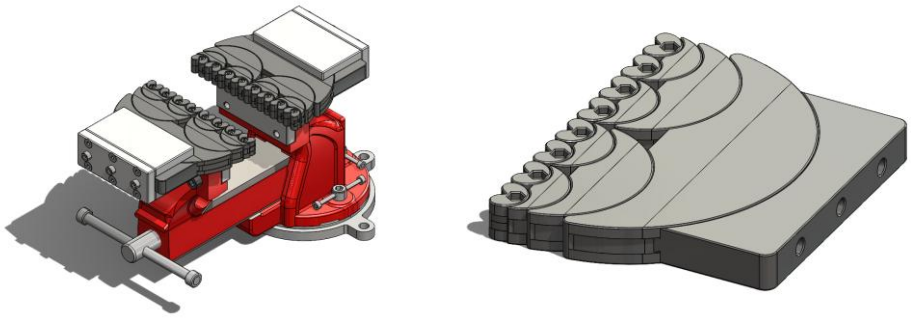

Picture 68. Model 2 of vise integration (left) and Fractal Vise (right) assemblies in SolidWorks - isometric view

Building upon this structural improvement, the next step is to numerically evaluate the performance of the component under the applied clamping conditions. Using finite element analysis (FEA), the is to assess how the reinforced configuration model behaves in terms of stress distribution and deformation. In particular, the results will be examined by comparing von Mises stress and total displacement values under several different studies scenarios, based on the type of fixture used and bolt connection model [25]. To perform accurate yet computationally efficient FEA simulations on SolidWorks, the vise integration assembly must be simplified onto the Fractal

Vise assembly, along with excluding fasteners and threaded inserts, analysing the mechanical behaviour of the fractal elements under load without excessive geometric complexity. From the table below, two types of fixtures are applicable to the project's model and application:

No.	Type of Fixture	Bolt Connection Model
1	The connecting part is rigid, and the fractal component is allowed to rise from the support surface. The indentation of the fractal bodies is not permitted into the support face. Displacement in the support plane (rigid virtual wall) is allowed.	Fix the hole surface (cylindrical surface) in every direction.
2	The connecting part is rigid, and the fractal component is allowed to rise from the support surface. The indentation of the fractal bodies is not permitted into the support face. Displacement in the support plane (rigid virtual wall) is allowed.	Fix the hole surface (cylindrical surface) in every direction – bottom holes of base plate. Interpret the effect of the bolt as a force in the local area under the bolt head – middle holes of base plate.

Before selecting fixtures and solving the studies, accurate input valus for pressure and bolt preload are essential for the FEA simulation:

- The clamping pressure represents the effect of the view jaw squeezing the workpiece. This is applied directly on the curved faces of the fractal segments.
- The bol preload describes the tension in the screws that attach the view jaws or the interface plate.

To calculate the pressure, the clamping force calculation using:

$$F = \frac{2\pi T * \eta}{d} = \frac{2\pi * 10 * 0.2}{0.00448} = 2804\ N$$

- T : Applied Torque = 10 Nm
- η : Efficiency factor = 0.2
- d : Lead or diameter of the screw mechanism = 5 mm = 0.005 mm (M5x16 screws)

Where the pressure value can be calculated using a general formula:

$$P = \frac{F}{A} = \frac{3769.9}{1848.27} = 1.5\ MPa$$

- A : Contact area = 1848.27 mm^2 (front surface of Part 2)

To accelerate the simulation of the FEA model and reduce computational demand, the full assembly was simplified by isolating the critical components – Part 1 and Part 2 – where the clamping force is applied and bending behaviour begins. These parts were combined into a single *SolidWorks* part file (since they share the same material) and then cut through the mid-plane using a *Surface Cut* to exploit symmetry, which halves the model size and retains the physical behaviour.

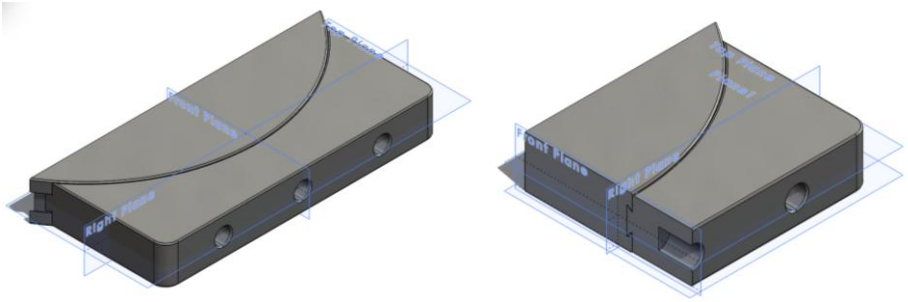

Picture 69. Simplify process of simulated models in SolidWorks – study 1

For material assignment, the intended PETG – CF was not available in the default library, so its mechanical properties were manually entered, and a custom material were created. The elastic modulus, Poisson's ratio, yield strength and density values were sourced from PETG – CF datasheets on the Material Selection Chapter and applied accordingly.

Property	Value	Units
Elastic Modulus	2020	N/mm^2
Poisson's Ratio	0.33	N/A
Shear Modulus	318.9	N/mm^2
Mass Density	2171.85	kg/m^3
Tensile Strength	50	N/mm^2
Compressive Strength		N/mm^2
Yield Strength	68.94	N/mm^2
Thermal Expansion Coefficient	6.8e-05	/K
Thermal Conductivity	0.2	W/(m·K)
Specific Heat	1350	J/(kg·K)
Material Damping Ratio		N/A

Picture 70. Custom material properties of PETG in SolidWorks

4.3.1 Simulation Study 1

After simplifying the assembly model, the initial simulation study was set up by defining a symmetry fixture at the cutting plane to represent the full-pattern geometry from the mirrored half. Two mid-planes were selected under the *Symmetry* fixture, enabling the solver to treat the model as if the other mirror body were present. Next, a *Fixed Geometry* fixture was applied to the mounting interface – specifically the inner surfaces of the M5 holes in Part 1 – to replicate the bolted connection to the base plate. A Virtual Wall was then defined on the bottom surfaces of both parts to allow the fractal bodies lift up from the support plate, as this might be a potential limitation factor during the application (e.g, bending on the first integration model).

On top of this, a pressure load of *0.5 MPa* was applied to the front surface of Part 2, as a result of reaction force of the clamped tool opposing the torque applied by the handle. For meshing, a *curvature-based mesh* strategy was adopted, specifying a minimum element size of *0.1 mm* and a maximum of *2 mm*. The resulting mesh comprised approximately 244,142 elements and 377,630 nodes, with an excellent quality metrics: 99.4% of elements had an aspect ration under 3, and no distorted elements were present.

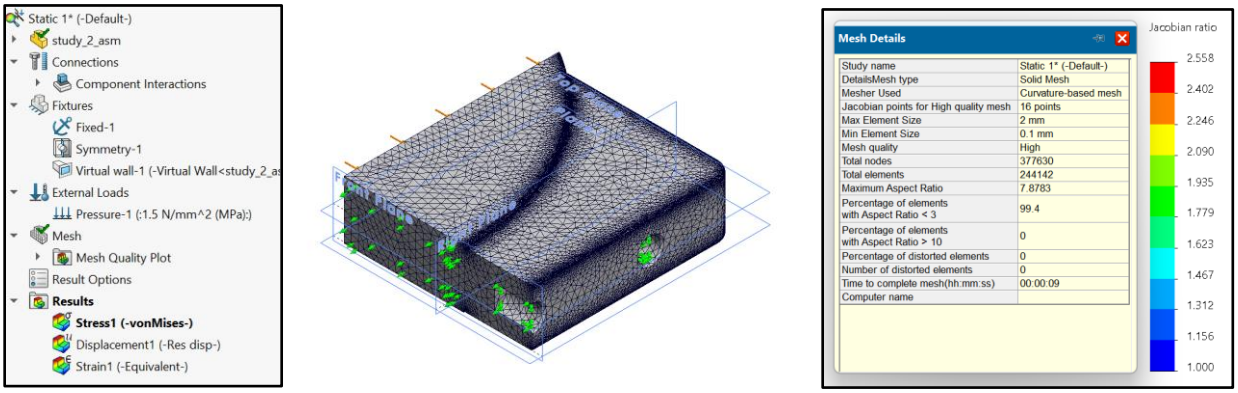

Picture 71. Simulation features (left) and mesh properties details (right) during simulation studies 1

The results of a finite element simulation is shown after clicking *Run This Study*. In the *von Mises* stress plot which represents in the left picture below, the minimum stress is approximately *0.002 MPa* and the maximum stress reaches around *31.203 MPa*. This value is far below the defined material yield strength of *68.94 MPa*, which means the component operates safely under the applied loading and is not expected to yield or fail. The higher stress zones appear around the

mounting and contact regions, where the clamping force and reaction forces are concentrated, especially new the fixed support.

The displacement plot (right picture) shows a maximum deformation of *0.17 mm* and a minimum of *0.0 mm*. The largest displacement occurs at the edge opposite the fixed or supported area, which is consistent with how materials flex under pressure. This value of deflection is relatively small and suggests the structure maintains its rigidity under the applied *1.5 MPa* pressure.

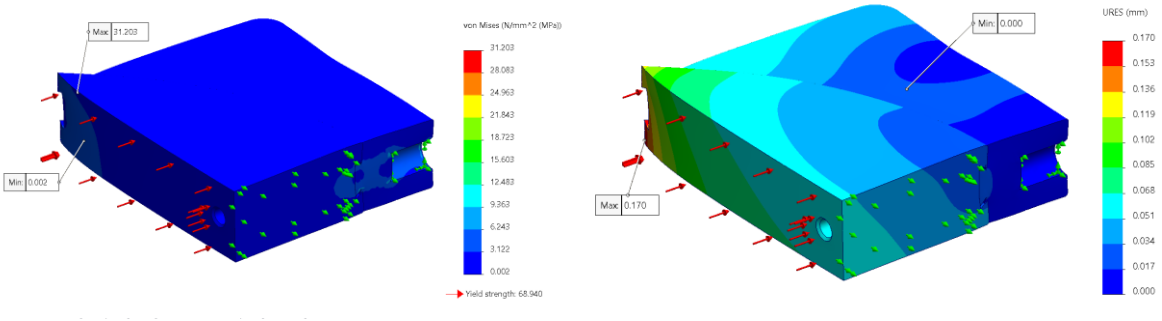

Picture 72. Von Mises stress (right) and displacement results - study 1

4.3.2 Simulation Study 2

Since the type of fixtures applied in the previous study is the same to this study, *Cyclic Symmetry*, *Virtual Wall*, and *1.5 MPa* pressure settings were also used. However, the *Fixed Geometry* was shifted to the inner surfaces of the bottom holes on the base plate, as this component is fixed and connected to the main supporting plate (Plate 2). Thus, *1000 N* of preload forces are applied for three bolts on the middle-plane holes, to interpret the effect of the bolt as a force in the local area under the bolt head. This preload forces are applied around the surface of base plate, specifically only under the head bolt area, thus force direction will be facing inner side of holes and clamping space. Here, the *split line* feature was used for the mounting interface plate to split the *Ø8.3 mm* area under the bolt's head (the mark can be seen in the right picture below). As these three bolts are placed via the vertical base plate, therefore another small assembly (display below) with an additional mounting plate part was added to exert the preload force to the simulation. Instead of using part file, the second study must be run under an assembly file due to different

material selection between the mounting interface and fractal bodies. Here, Alloy 1060 was chosen for the mounting interface, meanwhile PETG remained for the fractal bodies.

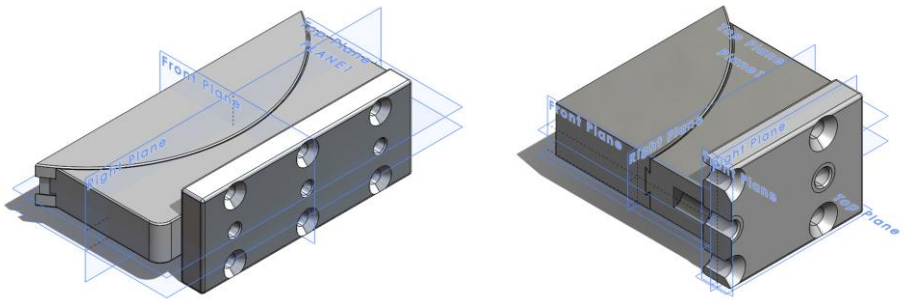

Picture 73. Simplify process of simulated models in SolidWorks – study 2

The same mesh setups were also used in this study: a *curvature-based mesh*, a *0.1 mm* minimum element size and a *2 mm* maximum element size; resulting in the same mesh details similar to the previous study. However, the results differ due to the more complex geometry and the inclusion of bolt preload features. The mesh quality remained high, with an aspect ration mostly under 3 and zero distorted elements. The total mesh includes 466,271 nodes and 30,1324 elements.

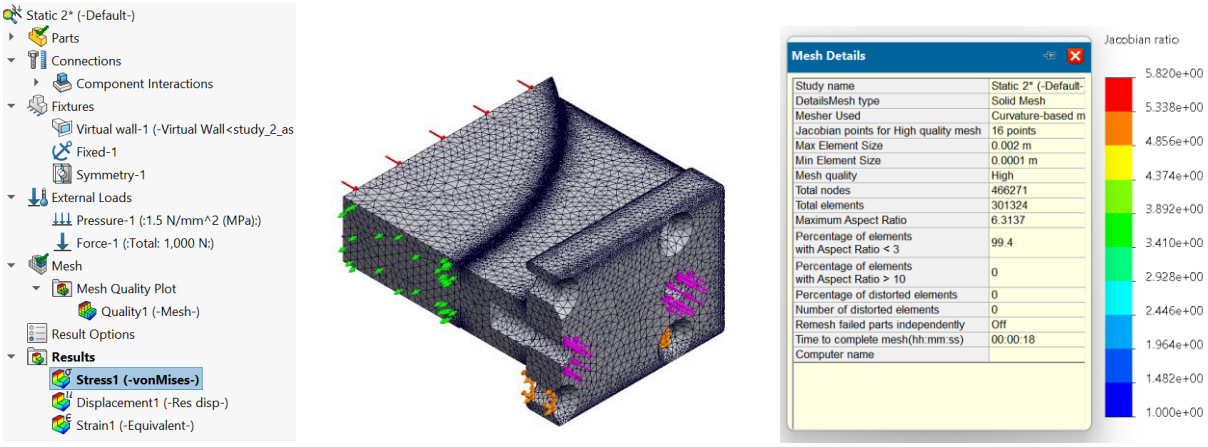

Picture 74. Simulation features (left) and mesh properties details (right) during simulation studies 2

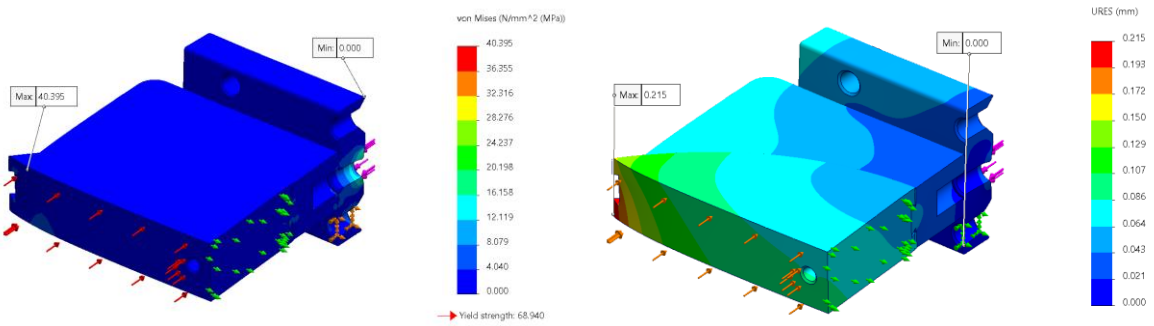

Picture 75. Von Mises stress (right) and displacement results - study 2

In the second study, the *von Mises* stress plot shows a maximum value of approximately *40.395 MPa* and a minimum *0 MPa* (near the fixed/support region). The displacement result indicates a maximum deflection of around *0.215 mm* and a minimum of *0 mm* (again at fixed supports). Because the peak stress is substantially below the material yield strength and the deflection remains very small, the model remains well within safe service limits. As the shape of the simplified model between Study 1 and Study 2 are different, the comparative analysis was analysed:

- The maximum stress increased from ~31 MPa in Study 1 to ~40.4 MPa in Study 2. This indicates that the changes in the moder or loading setup in Study 2 have resulted in a higher stress concentration (or redistributed load) compared to Study 1.
- The displacement also increased, from ~0.17 mm to ~0.215 mm, showing a slightly larger deformation under the condition of Study 2.
- Despite these increases, both stress and displacement remain at levels well below the material yield strength and deformation is still very small in absolute terms. That means the design is still safe and within acceptable limits for industrial application.
- The increase in stress and deformation may be due to the changed geometry, different boundary conditions or load path. When comparing simulation studies, slight changes in shape, mesh density, or constraints can cause noticeable shifts in stress/displacement values.

5. CONCLUSION

In this project, the design of the Fractal Vise model has been systematically advanced with the combination of Bench Vise function within the system. Limitations were indeed identified in the first assembly model – upward deflection of the bottom region of the fractal bodies under load - were successfully addressed by the optimized design, which was validated through side-view experimental testing showing no bending of the bottom parts. FEA evaluation confirmed these findings: von Mises stress levels remained well below material yield strength and displacements were minimal. This shows the type of vise model, specifically with the upgraded design is highly appropriate for use in maintenance shopfloor and assembly-line environments when paired with conventional vises such as Bench Vise and Machine Vise.

Within the context of Atlas Copco, the development of this vise was focused on improving clamping-tool efficiency for manual and light-machining tasks. Production cost was kept low as the material amount used for the manufacturing (additive and subtractive) manufacturing are little, yet the system demonstrated the capacity to handle large industrial tools – confirmed experimentally. A Bench Vise already available incurred no additional cost, so the implementation is straightforward into the assembly line where the function of vise mechanism was used and needed. Here, the Fractal Vise allows local operators to clamp various shapes and complex tools, thereby reducing setup time and installation footprint. A conservative estimate indicates a production-process time saving of approximately 15% - 20%, contributing to enhanced line throughput and space efficiency.

BIBLIOGRAPHY

[1]. Jiaxin Huang, Jian Shen, Yilin Zheng, Zhigong Song, “Fractal Gripper: Adaptive manipulator with mode switching,” (accessed on Sept 3rd 2025). [Online]. In: Cornell University, Computer Science and Robotics. Available: [2402.16057] Fractal Gripper: Adaptive manipulator with mode switching

[2]. Gabriele A. Losa, “The Fractal Geometry of Life,” (accessed on Sept 5th 2025). [Online]. In: Rivista di Biologia / Biology Forum, 102 (2009), pp. 29-60. Available: RB Losa

[3]. Allmath, “Fractals: Definition, Types, Examples, & Applications,” (accessed on Sept 7th 2025). [Online]. Available: https://www.allmath.com/geometry/fractal-geometry

[4]. Shea Gunther, “9 Amazing Fractals Found in Nature,” (accessed on Sept 10th 2025). [Online]. Available: 9 Amazing Fractals Found in Nature

[5]. Tran Thanh Tung and Tran Vu Minh, “Development of a Prototype Fractal Vise,” (accessed on Sept 12nd 2025). [Online]. In: International Journal of Mechanical Engineering and Robotics Research, Vol. 14, No. 1, (2025), pp. 11-12. Available: Development of a Prototype Fractal Vise

[6]. Engineers Edge, LLC, “Coefficient of Friction Equation and Table Chart,” (accessed on Sept 13th 2025). [Online]. Available: Coefficient of Friction Equation and Table Chart

[7]. Christopher Borge, “3D Print A Fractal Vise That Can Hold Odd Shapes,” (accessed on Sept 15th 2025). [Online]. Available: 3D Print A Fractal Vise That Can Hold Odd Shapes - Make:

[8] BubsBuilds, “Fractal Vise Jaws - Mechanical Bearings,” (accessed on Sept 17th 2025). [Online]. Available: Fractal Vise Jaws - Mechanical Bearings

[9]. Jiaxin Huang, Jian Shen, Yilin Zhemg, Yanbo Guo, and Zhigong Song, “A fractal gripper with switchable mode for geometry adaptive manipulation,” (accessed on Sept 17th 2025). [Online]. In: Sci Rep 15, 14657 (2025). Avaiable: https://doi.org/10.1038/s41598-025-98752-z

[10]. P. O'Brien, J. F. Kowalewski, C. C. Kessens and J. I. Lipton, "A Fractal Suction-Based Robotic Gripper for Versatile Grasping," (accessed on Sept 19th 2025). [Online]. In: IEEE Robotics and Automation Letters, vol. 9, no. 7, pp. 6208-6215, (July 2024), doi: 10.1109/LRA.2024.3401138. Available: A Fractal Suction-Based Robotic Gripper for Versatile Grasping | IEEE Journals & Magazine | IEEE Xplore

[11]. J. W. Burdick and M. Tisdale, "The Fractal Hand–I: A Non-anthropomorphic, but Synergistic, Adaptable Gripper," (accessed on Sept 22nd 2025). [Online]. In: 2024 IEEE International Conference on Robotics and Automation (ICRA), Yokohama, Japan, (2024), pp. 4162-4169, doi:

10.1109/ICRA57147.2024.10610687. Available: The Fractal Hand–I: A Non-anthropomorphic, but Synergistic, Adaptable Gripper | IEEE Conference Publication | IEEE Xplore

[12]. M. Tisdale and J. W. Burdick, "The Fractal Hand-II: Reviving a Classic Mechanism for Contemporary Grasping Challenges," (accessed on Sept 22nd 2025). [Online]. In: 2024 IEEE International Conference on Robotics and Automation (ICRA), Yokohama, Japan, (2024), pp. 4133-4139, doi: 10.1109/ICRA57147.2024.10611267.

[13]. M. O. Idris, K.M. Adeleke, I.K. Okediran, and T.I. Mohammed, "Design and Fabrication of a Modified Bench Vise for Comfortability and Productivity," (accessed on Sept 23rd 2025). [Online]. In: Adeleke University Journal of Engineering and Technology, Vol. 5, No. 1, (2022), pp. 01-07. Available: View of Design and Fabrication of a Modified Bench Vise for Comfortability and Productivity

[14]. Mr. R. Rupanawar, Mr. T. V. Daundkar, Mr. S. R. Tanpure, and Prof. V. V. Said Patil, "Design and Modification of Bench Vice by Increasing the Degrees of Freedom," (accessed on Sept 25th 2025). [Online]. In: GRD Journals- Global Research and Development Journal for Engineering, vol. 1, (11 October 2016), ISSN: 2455-5703. Available: GRDJEV01I110053_OK-libre.pdf

[15]. Spectrum Filaments, "THE FILAMENT PETG CF," (accessed on Sept 28th 2025). [Online]. Available: eng_tds_the_filament_petg_cf.pdf

[16]. Bambu Lab, "PETG-CF," (accessed on Oct 2nd 2025). [Online]. Available: Bambu_PETG-CF_Technical_Data_Sheet_V2.pdf

[17]. M. Viccica, M. Galati, F. Calignano, L. Iuliano, "An additively manufactured fractal structure for impact absorption applications," (accessed on Sept 30th 2025). [Online]. In: Procedia CIRP. 118, 793-798 (2023). Available: An additively manufactured fractal structure for impact absorption applications - ScienceDirect

[18]. Y. Sun, Y. Liu, F. Pancheri, T. C. Lueth, "LARG: A Lightweight Robotic Gripper With 3-D Topology Optimized Adaptive Fingers," (accessed on Sept 30th 2025). [Online]. In: IEEE/ASME Transactions on Mechatronics. 27, 2026-2034 (2022). Available: 2402.16057

[19]. Bikar Metals, "EN AW-1050A". [Online]. Available: Aluminium ::: EN AW-1050 A

[20]. Pinkham, Myra, "The future of aluminium manufacturing," (accessed on Oct 2nd 2025). [Online]. In: ProQuest, Redhill Vol. 32, Iss. 2, (Mar/Apr 2019): 21-23. Available: The future of aluminium manufacturing - ProQuest

[21]. Bambu Store, “Bambu Lab X1C 3D Printer,” (accessed on Oct 4th 2025). [Online]. Available: Bambu Lab X1C | Carbon Fiber 3D Printer | Bambu Lab Asia Store

[22]. TOS OLOMOUC s.r.o, “Tool-room milling machine FNGJ 40 A,” (accessed on Oct 8th 2025). [Online]. Available: Tool-room milling machine FNGJ 40 A - TOS Olomouc s.r.o.

[23]. Bridgeport, “SERIES 1 BRIDGEPORT MILL,” (accesses on October 11st 2025). [Online]. Available: Bridgeport® Series I Standard Knee Mill

[24]. Dina Rochman and Sergio Vásquez, “A Conceptual Framework Based on Fractal Geometry for Design, Modeling and Rapid Prototyping of Complex Geometric Shapes,” (accessed on Oct 15th 2025). [Online]. In: Computer-Aided Design and Applications, 10(2), pp. 307–319. https://doi.org/10.3722/cadaps.2013.307-319. Available: A Conceptual Framework Based on Fractal Geometry for Design, Modeling and Rapid Prototyping of Complex Geometric Shapes: Computer-Aided Design and Applications: Vol 10, No 2

[25]. Wojciech Macek, “Fractal analysis of the bending-torsion fatigue fracture of aluminium alloy,” (accessed on Oct 20th 2025). [Online]. In: Engineering Failure Analysis, vol. 99, (May 2019), pp. 97-107. Available: Fractal analysis of the bending-torsion fatigue fracture of aluminium alloy - ScienceDirect